Predicting lapses of attention with sleep-like slow waves.

Thomas Andrillon[1]*, Angus Burns[1], Teigane MacKay[1], Jennifer Windt[2] & Naotsugu Tsuchiya[1,3,4]

Affiliations:

1. School of Psychological Sciences, Turner Institute for Brain and Mental Health, Monash University, Melbourne 3168, Victoria, Australia.
2. Philosophy Department, Monash University, Melbourne 3168, Victoria, Australia.
3. Center for Information and Neural Networks (CiNet), National Institute of Information and Communications Technology (NICT), Suita, Osaka 565-0871, Japan
4. Advanced Telecommunications Research Computational Neuroscience Laboratories, 2-2-2 Hikaridai, Seika-cho, Soraku-gun, Kyoto 619-0288, Japan.

*** Corresponding author:** Thomas Andrillon.

Postal Address: Monash Biomedical Imaging, 770 Blackburn Road, Clayton 3168, Victoria, Australia.

Email: thomas.andrillon@monash.edu

ORCID: https://orcid.org/0000-0003-2794-8494

Data and Code Availability:

Raw data: https://osf.io/ey3ca/?view_only=680c39e7065649c3b783a4efec0a1a94

Code used for analyses: https://github.com/andrillon/wanderIM

This file includes:

Main Text

Figures 1 to 6

Abstract

Attentional lapses are ubiquitous and can negatively impact performance. They correlate with mind wandering, or thoughts that are unrelated to ongoing tasks and environmental demands. In other cases, the stream of consciousness itself comes to a halt and the mind goes blank. What is happening in the brain that leads to these mental states? To understand the neural mechanisms underlying attentional lapses, we cross-analysed the behaviour, subjective experience and neural activity of healthy participants performing a task. Random interruptions prompted participants to indicate their mental states as task-focused, mind-wandering or mind-blanking. High-density electroencephalography revealed the occurrence of spatially and temporally localized slow waves, a pattern of neural activity characteristic of the transition toward sleep. These slow waves accompanied behavioural markers of lapses and preceded reports of mind wandering and mind blanking. Furthermore, the location of slow waves distinguished sluggish versus impulsive behaviours, mind wandering versus mind blanking. Our results suggest attentional lapses share a common physiological origin: the emergence of local sleep-like activity within the awake brain.

53 # Introduction

54 The human brain sustains the stream of our conscious experiences. Attention can direct
55 cognitive resources toward the external world and enable the selection and amplification
56 of information relevant to an individual's current behavioural goals[1]. But attention can also
57 turn inward, as is the case when we focus on internally generated task-unrelated thoughts,
58 a phenomenon usually referred to as mind wandering[2]. Recent investigations have also
59 shown that the stream of thoughts can come to a pause, as when individuals who are awake
60 are left with the feeling of an empty mind (mind blanking)[3].

61 Shifts of attention towards the internal world, invoking mind blanking and mind
62 wandering, can occur spontaneously without our knowledge or will[4]. In fact, a
63 characteristic feature of attention is its fleeting nature and the difficulty to maintain it on a
64 task for long periods of time[1,5]. In this paper, we define lapses of attention as the shift of
65 the focus of thoughts away from the task at hand or environmental demands. The
66 consequences of attentional lapses are very diverse. At the behavioural level, they can
67 result in a lack of responsiveness or sluggish reactions, but they can also result in impulsive
68 responses[6]. Curiously, these behavioural failures can be accompanied by a lack of
69 conscious awareness and the absence of mental activity (mind blanking[3]), or rich,
70 spontaneous mental activity (mind wandering[2]).

71 It is yet unclear whether these different types of attentional lapses (sluggish vs. impulsive
72 behaviours; mind-blanking vs. mind-wandering) belong to a disparate family of
73 behavioural and phenomenological events[7,8], each of them associated with different
74 physiological causes,[9,10] or whether they can be traced back to common underlying

physiological causes[11]. Previous models of mind wandering have proposed that mind wandering and mind blanking might arise in distinct neurophysiological states[3,9,10]. However, the fact that both sluggish and impulsive responses increase following sleep deprivation[12,13] and in individuals with attentional deficits[6,14] implies a common mechanism. Likewise, sleepiness has been associated with both mind wandering and mind blanking[15,16] despite these two mental states being phenomenologically distinct[3]. Furthermore, investigations of the sleep onset period (hypnagogia) indicate that subjective experiences resembling mind wandering (focus on internally generated contents) and mind blanking (loss of awareness) can both occur at the border between wakefulness and sleep[17,18]. Interestingly, these studies seem to associate lapses with pressure for sleep, suggesting an involvement of fatigue.

Indeed, each hour spent awake comes at the cost of mounting sleep pressure. Past research suggests that the need for sleep might only be dissipated by sleep itself,[19] as sleep plays a vital role in neural homeostasis[20]. When individuals are prevented from sleeping for extended periods of time (as in sleep deprivation studies), a subset of brain regions can start displaying electroencephalographic (EEG) signatures of non-rapid eye-movement (NREM) sleep in the form of sleep-like slow waves (within the delta (1-4 Hz) or theta (4-7 Hz) range), despite individuals being behaviourally and physiologically awake[21,22]. These sleep-like slow waves within wakefulness are referred to as “local sleep” in contrast with the global whole-brain transition commonly observed at sleep onset[22–25]. Importantly, both local and global transitions toward sleep are characterised by the same neural signature: the occurrence of high-amplitude slow waves.

It has been proposed that the multiplication of sleep-like slow waves could perturb brain

98 functions and cause behavioural lapses[22]. In fact, during sleep, slow waves are associated
99 with episodes of widespread neural silencing[26], which have been connected to sensory
100 disconnection, behavioural unresponsiveness and the loss of consciousness[27,28].
101 Intracranial studies in humans and rodents showed that slow waves during waking are
102 associated with reduced neuronal firing, resulting in behavioural errors[21,22]. Wake slow
103 waves can also be detected in human non-invasive recordings[29–31] and here again the
104 amount of slow waves recorded in a given brain region correlates with the number of errors
105 performed in a task recruiting this specific brain region[29,30]. These results strongly suggest
106 that slow waves could explain the behavioural component of attentional lapses[22]. However,
107 the impact of slow waves on conscious experience, including mind wandering and
108 blanking, is still unclear.

109 In a recent review, we proposed that local sleep, manifested as the occurrence of slow
110 waves in waking, could not only explain the behavioural consequences of attentional
111 lapses, both regarding sluggish and impulsive responses, but also their phenomenology,
112 like mind wandering or blanking[11]. We also argued that local sleep is not an extreme
113 phenomenon, occurring only when individuals are pushed to their limit, but could occur in
114 well-rested individuals[31] and explain the occurrence of lapses in our everyday lives. To test
115 this framework, we rely on the detection of slow waves and formulate three different
116 hypotheses as follows: (i) Can slow waves predict, at the single trial level, both sluggish
117 and impulsive behaviours in well-rested individuals? (ii) Are slow waves associated with
118 both mind wandering and blanking? (iii) Does the location of slow waves (i.e. which
119 electrodes show slow waves) differentiate between sluggishness and impulsivity, mind-
120 blanking and mind-wandering? Through these hypotheses we will test the idea that local

slow waves could act as a functional switch, transiently perturbing the functioning of a given cortical network. Accordingly, a common physiological event (local slow waves) could lead to drastically different outcomes depending on its location within the brain.

To test these hypotheses, we cross-examined the behavioural performance, subjective reports and physiological data from healthy individuals (N=26) performing an undemanding Go/NoGo tasks[32] (Figure 1a). We sampled participants' subjective experience by interrupting them during the task and asking them a series of questions about their mental states prior to the interruption, including whether they were focusing on the task, mind-wandering or mind-blanking (Figure 1b). Finally, we recorded their brain activity using high-density scalp EEG and pupil size as objective proxies for participants' level of vigilance[33]. Importantly, here participants were neither sleep deprived nor placed in conditions favouring dozing off (i.e. not in bed or reclined, task requiring constant attention and responses).

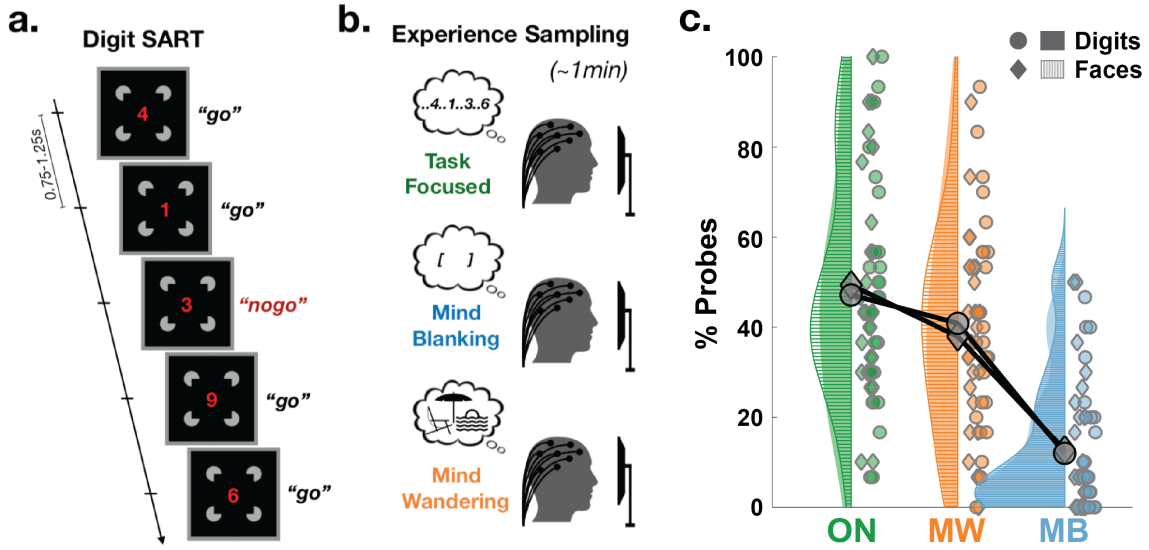

Figure 1. Experimental design and hypotheses.

a: *Participants performed both a SART on faces stimuli (NoGo trials: smiling faces, stimuli*

shown because of BioRxiv's guidelines) and a SART on digits (NoGo trials: "3"). Face/Digit presentation was continuous (new face/digit every 0.75-1.25s). ***b:*** *Every 30 to 70s, participants were interrupted and instructed to report their mental state (see Online and Supplementary Methods). Most importantly, they were asked to indicate whether they were focusing on the task (task-focused: ON), thinking about nothing (mind-blanking: MB) or thinking about something other than the task (mind-wandering: MW). High-density EEG and pupil size were continuously recorded throughout the task.* ***c:*** *Proportion of mental states reported during probes categorized as task-focused (ON, green), mind-wandering (MW, orange) and mind-blanking (MB, blue) during the tasks with Digits (circles for each individual participant; filled surfaces for smoothed density plot) and Faces (diamonds and surfaces with horizontal stripes). Grey diamonds and circles show the average across participants.*

Results

Task performance and subjective experience. The Go/NoGo tests (see Online Methods) require participants' sustained attention, but our participants declared focusing on the task only in ~48% of the probes (Face Task: 49.4 ± 4.9%; Digit Task: 47.2 ± 5.1%; mean ± Standard Error of the Mean (SEM) across N=26 participants; Figure 1c). The rest of the time, they declared thinking about something else (Mind Wandering (MW); Face: 38.0 ± 4.3%; Digit: 40.9 ± 4.8%; Figure 1c) or thinking about nothing (Mind Blanking (MB); Face: 12.7 ± 3.0%; Digit: 11.9 ± 2.9%; Figure 1c). These results are well in line with previous findings[34,35] and highlight the prevalence of attentional lapses. Attentional lapses were also reflected in participants' accuracy on the Go trials (Face: 3.1 ± 0.4% of miss, i.e., errors on Go trials; Digit: 1.7 ± 0.2%; Figure 2a), but more notably on the NoGo trials (Face: 35.0 ± 2.5% of false alarms (FA), i.e., errors on NoGo trials; Digit: 32.5 ± 2.7%; Figure 2b).

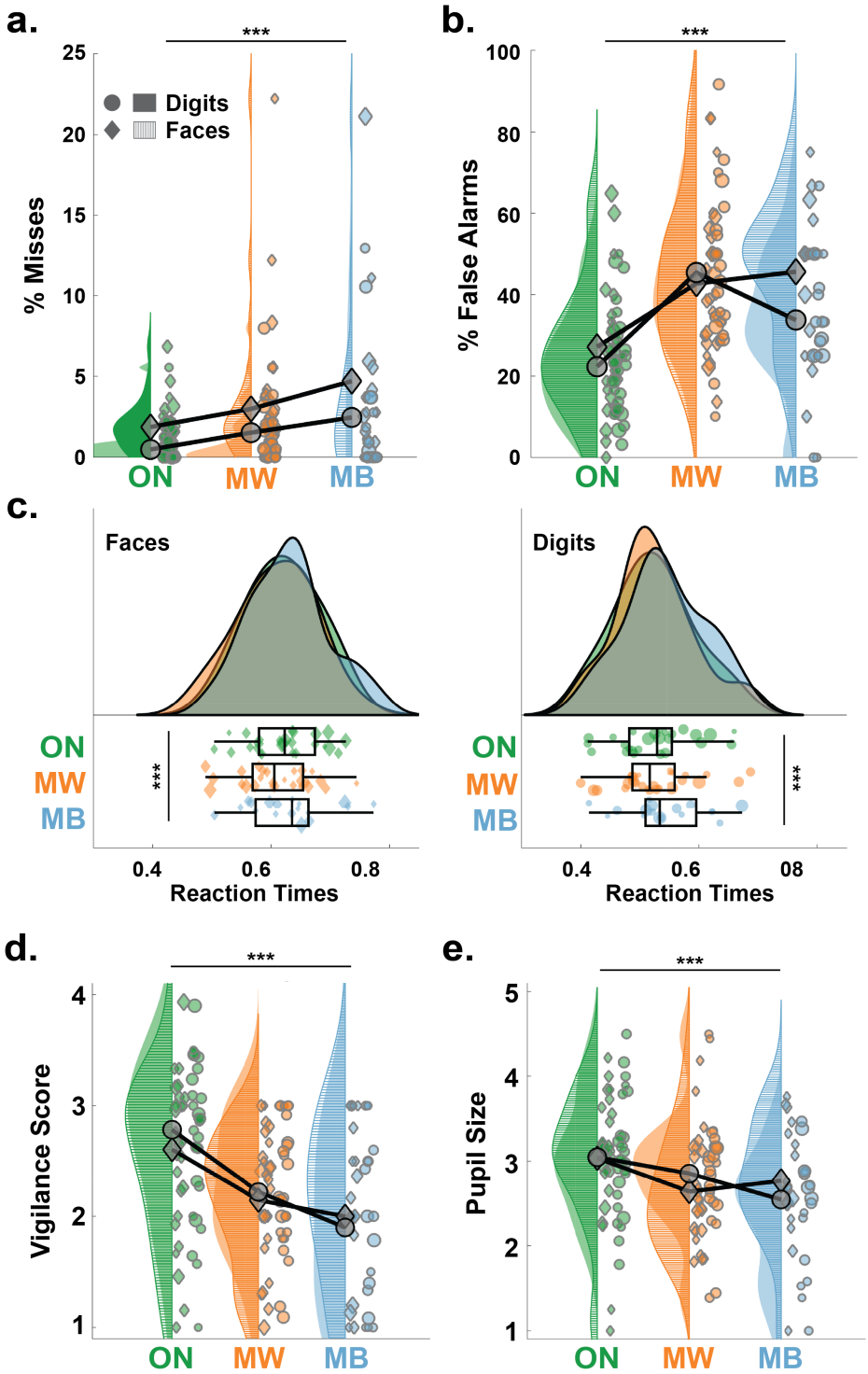

Figure 2. Low arousal is associated with attentional lapses characterized by different behavioural outcomes

*Proportion of misses (**a**) and false alarms (**b**) in the 20s preceding task-focused (ON, green), mind-wandering (MW, orange) and mind-blanking (MB, blue) during the tasks with*

*Digits (circles for each individual participant; filled surfaces for smoothed density plot) and Faces (diamonds and surfaces with horizontal stripes). The markers' size is proportional to the number of reports for each participant (same for **c-e**). Grey diamonds and circles show the average across participants, weighted by the number of reports (same for **c-e**). **c:** Distribution of reaction times (RT) for Go Trials (left: Face; right: Digit) in the 20s preceding ON, MW and MB reports. Box plots show the mean (central bar), the lowest and highest individual data points (end of the whiskers) and the lower and higher quartiles (edges of the box). On top of each plot are shown the smoothed density plot for the different mental states. **d:** Vigilance scores (subjective ratings provided during probes) associated with ON, MW and MB reports. **e:** Discretized pupil size (see Online Methods) in the 20s preceding ON, MW and MB reports. In **a-e**, stars show the level of significance of the effect of mental states (Likelihood Ratio Test, see Online Methods; ***: p<0.005).*

Next, we focused on the behavioural patterns preceding subjective reports of attentional lapses. Specifically, we examined participants' behaviour in the 20s before the onset of the probes that led to MW and MB reports (see Online Methods). To quantify the impact of mental states (i.e., ON, MW or MB) on behaviour, we compared statistical models that either did or did not include mental states as a predictor of behaviour (see Online Methods and Supplementary Table 1). A significantly better fit by the model incorporating mental states, assessed through a Likelihood Ratio Test, was interpreted as evidence for the influence of mental states. To describe the size and direction of the statistical effects, we report the estimates (β) of the contrasts of interest (MW vs ON, MB vs ON and MB vs MW) and their 95% confidence-interval (CI). Accordingly, we found a significant effect of mental states on misses (model comparison: $\chi^2(2)=36.0$, $p=1.5\times10^{-8}$; Figure 2a). Specifically, MW and MB were associated with an increase in misses compared to ON reports (MW vs ON: β=0.011, CI: [0.005, 0.016]; MB vs ON: β=0.023, CI: [0.015, 0.032]) and misses were more frequent for MB compared to MW reports (MB vs MW: β=0.013,

194 CI: [0.005, 0.021]). False alarms were also modulated across mental states (model
195 comparison: $\chi^2(2)=115.9$, $p<10^{-16}$; see Figure 2b), with an increase for both MW and MB
196 compared to ON (MW vs ON: β=0.21, CI: [0.17, 0.24]; MB vs ON: β=0.17, CI: [0.12,
197 0.23]), but similar levels of false alarms for MB and MW (MB vs MW: β=-0.028, CI: [-
198 0.084, 0.028]). Finally, mental states were associated with different patterns of reaction
199 times (RT; model comparison: $\chi^2(2)=16.3$, $p=2.9\times10^{-4}$; Figure 2c) with slower reaction
200 times for MB compared to both ON and MW reports (MB vs ON: β=0.019, CI: [0.009,
201 0.030]; MB vs MW: β=0.022, CI: [0.011, 0.032]; MW vs ON: β=-0.0025, CI: [-0.0096,
202 0.0045]).

203 Taken together, these results suggest that MW and MB decrease performance in different
204 ways. MB is characterized with more misses and slower RT than MW and ON, which is
205 consistent with the idea that MB induces sluggish mental states. As to MW, the analysis of
206 misses may ostensibly compatible with an idea of MW as a mild form of MB, however,
207 the fact that RT in MW is faster than in MB is not easy to reconcile with such an idea.
208 Instead, this overall pattern is consistent with an idea that MW induces more impulsive
209 mental states.

210 The same pattern of results was obtained when normalising misses, false alarms and RT in
211 the MW and MB conditions by the average obtained in the ON condition for each subject
212 (see Supplementary Table 2). We also obtained qualitatively the same results when
213 focusing on a shorter time-window (10s before probe onsets instead of 20s; see
214 Supplementary Table 3).

215 **Vigilance.** Although MW and MB differ according to their phenomenological definition
216 and associated behaviours, both states seem to occur in a similar context of low vigilance

217 (as reported by participants themselves during probes). To address this, we quantified the
218 degrees of correlation between participants' vigilance ratings and each mental state
219 (comparison between models including or not the information about mental state:
220 $\chi^2(2)=144.8$, $p<10^{-16}$; Figure 2d and Supplementary Table 1). Participants reported lower
221 vigilance ratings for both MW and MB compared to ON (MW vs ON: $\beta=-0.39$, CI: [-0.40,
222 -0.37] and MB vs ON: $\beta=-0.53$, CI: [-0.55, -0.50]). Vigilance ratings were even lower for
223 MB compared to MW (MB vs MW: $\beta=-0.13$, CI: [-0.24, -0.02]). We then examined a
224 classical objective proxy for vigilance: pupil size[33,36]. Pupil size prior to probes (Figure 2e,
225 N=25 participants here, see Online Methods) was significantly modulated by mental states
226 (model comparison: $\chi^2(2)=18.0$, $p=1.210^{-4}$) with MW and MB associated with smaller
227 pupils than ON probes (MW vs ON: $\beta=-0.29$, CI: [-0.43, -0.15]; MB vs ON: $\beta=-0.22$, CI:
228 [-0.45, -0.003]). Pupil size did not differ between MW and MB (MB vs MW: $\beta=0.065$, CI:
229 [-0.16, 0.29]), despite the significant correlation between vigilance ratings and pupil size
230 (model comparison: $\chi^2(2)=134.5$, $p<10^{-16}$; see Table S1 for details on the models). This
231 implies that these two measures of vigilance can be differentially sensitive to mental states.

232 **Slow Waves.** To further examine the potential mechanistic link between sleep pressure and
233 attentional lapses, we set out to detect a marker of sleep pressure in the EEG signal, in the
234 form of local, sleep-like slow waves. We recently reviewed the rationale behind this
235 approach[11]. In particular, relying on a local marker of sleep allowed us to test whether
236 distinct families of attentional lapses can be coherently explained by the occurrence and
237 spatio-temporal characteristics of slow waves.

238 Following evidence from [21,22,29,30], we operationally defined slow waves as the occurrence
239 of large-amplitude waves within the delta ([1-4] Hz) range. We first detected the

occurrence of slow waves in each EEG electrode using an established approach developed in wakefulness and sleep (see [30,31,37] and Online Methods). Both the temporal profile and topographical distribution of slow waves detected during the tasks (Figure 3a-b) resemble the slow waves observed in NREM sleep[37,38]. This is not trivial as our detection algorithm did not select this specific temporal profile or topographical distributions.

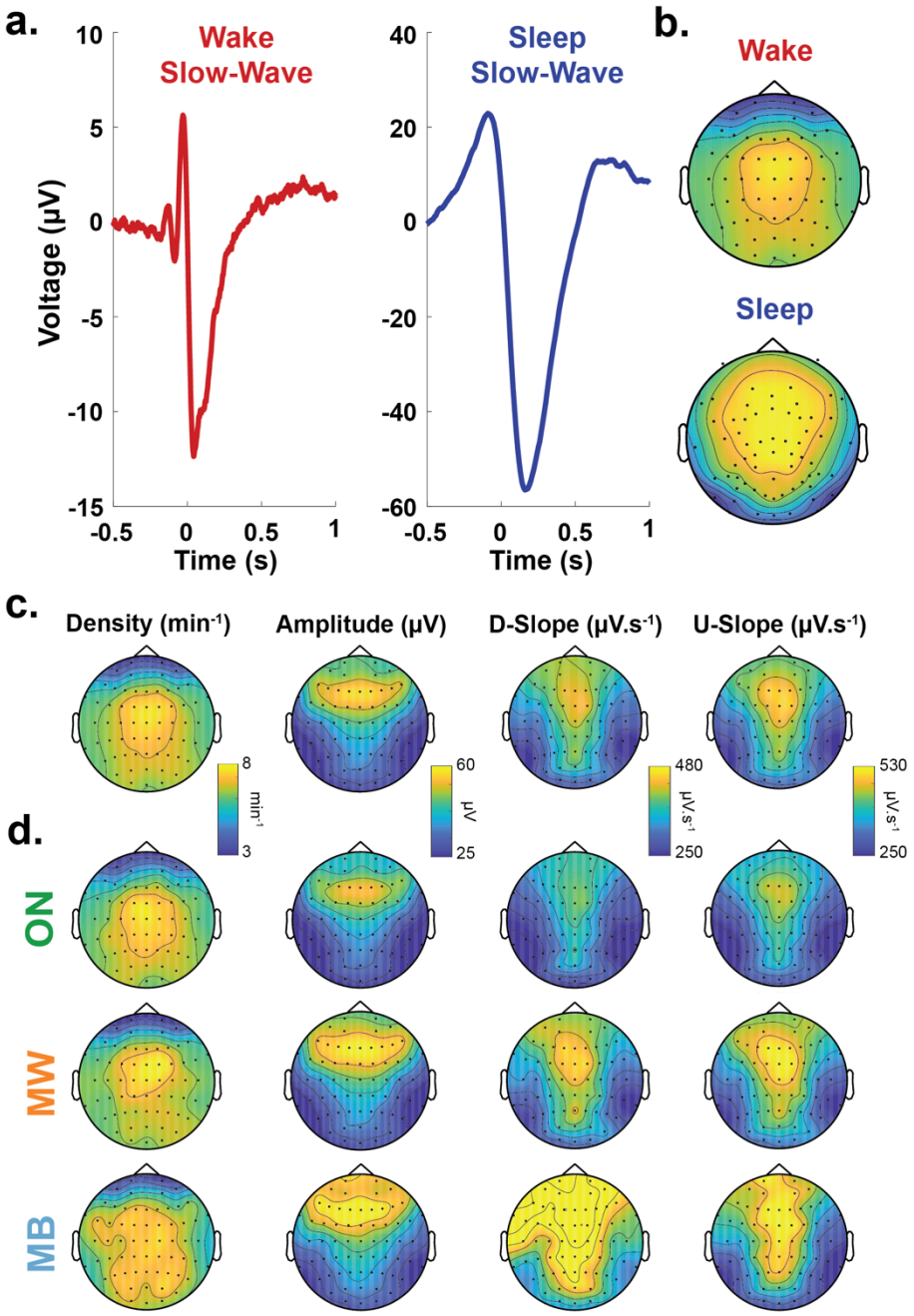

Figure 3. Properties of Slow Waves

a: *Average waveform of the slow waves detected over electrode Cz during the behavioural tasks (red, left; N=26 participants). The average waveform of slow waves detected during sleep (blue, right), extracted from another dataset (see Supplementary Methods), is shown for comparison. Slow waves were aligned by their start, defined as the first zero-crossing before the negative peak (see Online Methods).* ***b:*** *Scalp topographies of the density of slow waves (arbitrary units) detected in wakefulness (top) and sleep (bottom).* ***c:*** *Scalp topographies of wake slow-waves properties (1st column: temporal Density; 2nd: peak-to-peak Amplitude; 3rd: Downward Slope (D-Slope); 4th: Upward Slope (U-Slope); see Online Methods) averaged across participants (N=26).* ***d:*** *Scalp topographies for slow-waves Density (1st column), Amplitude (2nd), Downward Slope (D-Slope, 3rd) and Upward Slope (U-Slope, 4th) for the different mental state (ON, MW and MB).*

Relationship between global properties of slow waves and vigilance. Next, we checked whether global properties of the slow waves index participants' level of vigilance. We correlated first participants' subjective vigilance ratings with the amount and properties of slow waves. The amount and properties of slow waves were extracted prior to probe onset ([-20, 0]s) and averaged across the entire scalp (all 63 electrodes, see Online Methods). Model comparisons between models with or without slow-wave density, amplitude, downward slope or upward slope indicate a negative correlation between vigilance ratings and slow-waves density ($\chi^2(1)=13.1$, $p=3.9\times10^{-4}$, $\beta=-0.074$, CI: [-0.114, -0.034]), amplitude ($\chi^2(1)=33.1$, $p=8.5\times10^{-9}$, $\beta=-0.023$, CI: [-0.031, -0.015]), downward slope ($\chi^2(1)=82.1$, $p<10^{-16}$, $\beta=-2.5\times10^{-3}$, CI: [-3.1×10^{-3}, -2.0×10^{-3}]), and upward slope ($\chi^2(1)=47.3$, $p<10^{-11}$, $\beta=-1.7\times10^{-3}$, CI: [-2.2×10^{-3}, -1.2×10^{-3}]) (see also Figure S1). We then verified that slow-wave properties were negatively correlated with pupil size recorded before each probe (model comparison between models with or without slow-wave density, amplitude, downward slope or upward slope: density: $\chi^2(1)=12.3$, $p=4.6\times10^{-4}$, $\beta=-0.13$, CI:

272 [-0.21, -0.059]; amplitude: $\chi^2(1)=7.4$, $p=6.4x10^{-3}$, $\beta=-0.0088$, CI: [-0.015, -0.0025];
273 downward slope: $\chi^2(1)=15.1$, $p=1.0x10^{-4}$, $\beta=-6.9x10^{-4}$, CI: [$-1.0x10^{-3}$, $-3.4x10^{-4}$]; upward
274 slope: $\chi^2(1)=17.6$, $p=2.7x10^{-5}$, $\beta=-7.6x10^{-4}$, CI: [$-1.1x10^{-3}$, $-4.0x10^{-4}$]) (see also Figure S2).
275 Finally, we confirmed that the amount of slow waves detected increased with time spent
276 on task (Figure S3), as can be expected when considering the homeostatic regulation of
277 sleep and local sleep[22].

278 *Relationship between local properties of slow waves and mental states at the probe level.*
279 Local properties of the slow waves (Figure 3c-d) predicted reports of mental states.
280 Specifically, we examined, for each scalp electrode, whether slow-wave properties
281 (density, amplitude, downward and upward slopes) prior to probes were predictive of the
282 mental state reported by participants. To do so we focused on pairwise contrasts (MW vs
283 ON, MB vs ON and MB vs MW) and performed this analysis for each electrode
284 independently. A cluster permutation approach ($p_{cluster}<0.05$, Bonferroni corrected cluster
285 threshold; see Online Methods) revealed that MW (compared to ON) was predicted by an
286 increase in the number of slow waves and slow wave amplitude over frontal electrodes,
287 and by an increase in slow waves' downward and upward slope over centro-frontal
288 electrodes (Figure 4a). MB (compared to ON; Figure 4b) was also predicted by an increase
289 in slow wave density over frontal areas as well as by the slow-wave slopes (downward and
290 upward) over centro-parietal electrodes (no significant cluster for slow wave amplitude).
291 Finally, a direct contrast between MB and MW (Figure 4c) indicated that a reduction of
292 slow wave amplitude over frontal electrodes but an increase in their upward slope over
293 parietal electrodes were predictive of MB. No significant clusters were obtained for slow
294 wave density and downward slope.

To provide more details on the temporal relationship between slow waves and mental states, we replicated this analysis by splitting the 20s window before probes into four windows of 5s (Figure S4-6). The contrasts between MW and ON (Figure S4) as well as MB and ON (Figure S5) show that the properties of slow waves best predict mental states within the 5s before a probe. In terms of topography, when compared to ON state, MW is best predicted by the slow wave properties in frontal electrodes (Figure S4) while MB is best predicted by those in the centro-parietal electrodes (Figure S5).

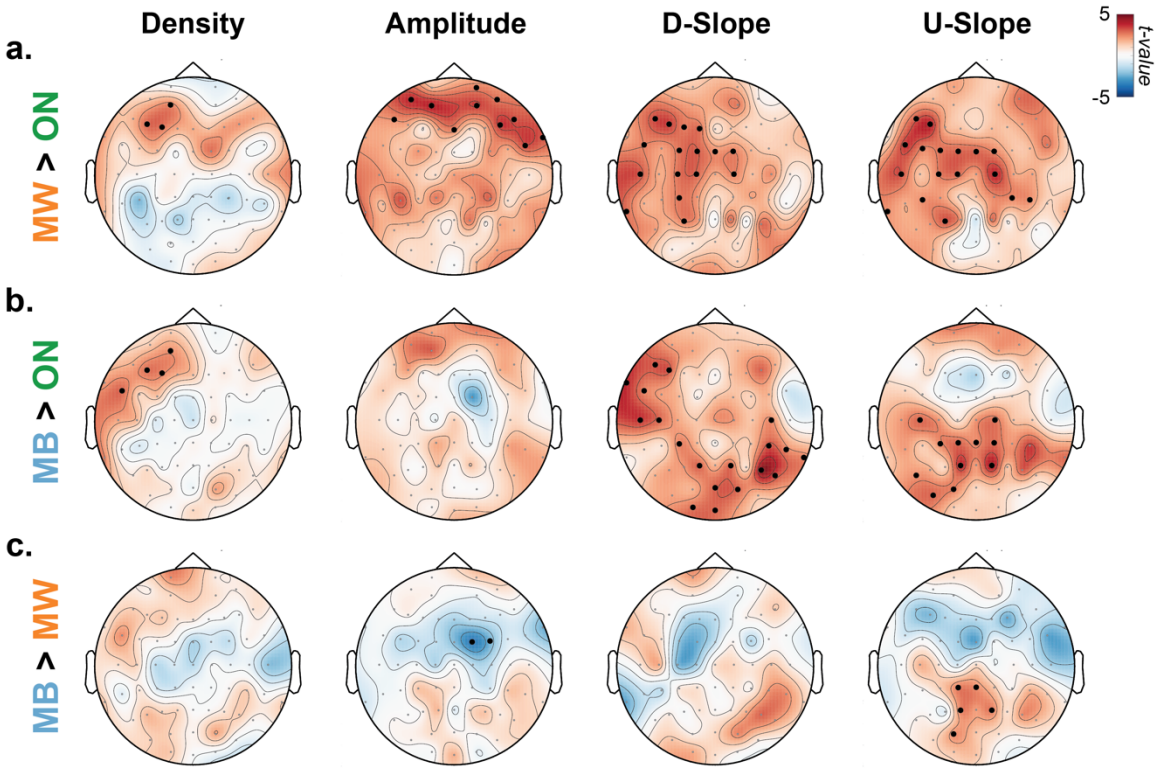

Figure 4. Local properties of slow waves are predictive of mental states

Locally, based on each individual electrode, we performed mixed-effect analyses, following with permutation analysis to quantify the impact of slow wave properties on mental states. 1st column: Density; 2nd: Amplitude; 3rd: Downward Slope (D-slope); 4th: Upward Slope (U-slope). These slow-wave properties were extracted for each electrode and used to compute the t-values (shown in each topographical plot) from t-tests on the following comparisons: (a) MW > ON (b) MB > ON and (c) MB > MW. Black dots denote

significant clusters of electrodes ($p_{cluster}$<0.05 corrected for 12 comparisons using a Bonferroni approach, see Online Methods).

Relationship between local properties of slow waves and behaviour at the trial level. To further understand the association between slow waves and attentional lapses, we examined the influence of slow waves on participants' behaviour at the single-trial level (for all trials within 20s of a probe onset, independently of mental states). To do so, for each trial and electrode, we marked the presence or absence of slow waves between stimulus onset and offset (see Online Methods) and used this as a (binary) predictor of RT, misses and false alarms (Figure 5). This analysis revealed spatially-specific effects of slow waves on distinct behavioural outcomes. Namely, slow waves in frontal electrodes co-occurred with faster reaction times while slow waves in posterior electrodes co-occurred with slower reaction times (Figure 5a, $p_{cluster}$<0.05, Bonferroni corrected cluster threshold). Likewise, frontal slow waves were associated with more false alarms (a marker of impulsivity, Figure 5b) and posterior slow waves with more misses (a marker of sluggishness, Figure 5c).

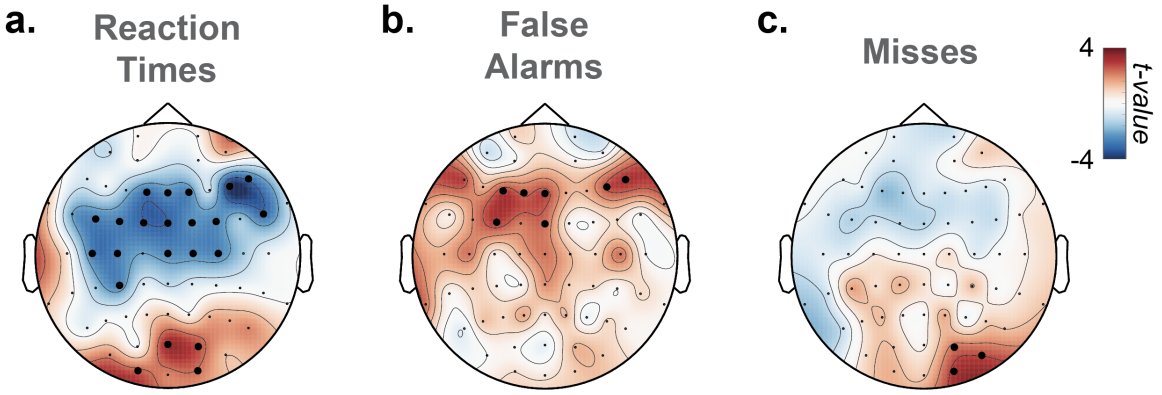

Figure 5. Local occurrences of slow waves are associated with modulations of performance

Mixed-Effects Models were used to quantify the correlation between slow-wave occurrence

329 *and reaction times (**a**), false alarms (**b**) and misses (**c**) at the single-trial level.*
330 *Topographies show the scalp distribution of the associated t-values. Black dots denote*
331 *significant clusters of electrodes ($p_{cluster}$<0.05 corrected for 3 comparisons using a*
332 *Bonferroni approach, see Online Methods).*

333 **Decision modelling.** Finally, we implemented an influential model of two-alternative
334 forced-choice (2AFC) decision making: the diffusion decision model (DDM)[39]. The DDM
335 decomposes full reaction-time distributions and choice proportions into latent cognitive
336 processes that are thought to underlie participants' decisions in 2AFC tasks (see Online
337 and Supplementary Methods and Figure S7). These include the time it takes for participants
338 to start computing their response (Non-Decision Time or NDT [t]), the speed at which
339 participants accumulate evidence for the two responses (drift rates for Go [v_{Go}] and NoGo
340 [v_{NoGo}] responses), the amount of evidence needed to reach a decision (decision threshold
341 [a]), the participants' initial bias for one of the two responses (decision bias [z]) and the
342 bias for the accumulation of evidence for one of the two responses (drift bias, [v_{Bias}]). A
343 hierarchical Bayesian approach was used to fit the DDM to the reaction times obtained in
344 the Go/NoGo tests[40] so that each parameter (v_{Go}, v_{NoGo}, a, z, t and v_{Bias}) was free to vary by
345 participant, task and mental states (ON, MW and MB) or slow-wave occurrence (present
346 vs. absent). Simulations confirmed this hierarchical DDM can successfully predict the
347 observed data (Figure S8).

348 Considering the trials that were within 20 seconds from the onset of the probes, we first
349 estimated these different parameters of the DDM for each mental state (Figure S9). This
350 analysis shows differences between MW and MB reports in terms of decision bias and
351 threshold (Figure S9). The lower threshold and higher decision bias observed for MW
352 (compared to MB) are concordant with the idea that MW is associated with behavioural

353 impulsivity.

354 We then used this modelling approach to examine how the occurrences of slow waves
355 impact the different cognitive processes leading to participants' responses, with a particular
356 focus being the test of our core hypothesis: the presence of slow waves in frontal areas
357 leads to impulsivity by disrupting the cognitive mechanisms underlying executive control,
358 while the presence of slow waves in posterior areas leads to sluggishness by slowing down
359 the integration of sensory inputs.

360 We report here the differences in the parameters' estimates in the presence or absence of
361 slow waves detected for each electrode (Figure 6). The associated scalp topographies
362 indicate both global and local (electrode-specific) effects of slow waves on DDM
363 parameters. As global effects (Figure 6d-f), we found first that the presence of slow waves
364 was associated with a reduction in decision threshold (*a*; Figure 6d), consistent with the
365 idea that slow waves facilitate impulsive responses. Second, slow waves were also
366 associated with longer non-decision times (*t*; Figure 6e), suggesting that slow waves can
367 slow down neural processes underlying stimulus encoding and/or motor preparation.
368 Finally, the presence of slow waves was correlated with an increase in the starting point of
369 the decision process (prior bias *z*; Figure 6f), implying shifts in the decision process
370 towards Go responses.

371 As local electrode-specific effects, we observed again contrasting results between posterior
372 and frontal slow waves (Figure 6a-c). Slow waves within posterior electrodes were
373 associated with a reduction of v_{Go} and v_{Bias}, meaning that evidence accumulation was
374 slower for Go decisions and the drift bias of the decision process for Go responses was
375 reduced (Figure 6a,c). Conversely, slow waves within frontal electrodes correlated with a

reduction of v_{NoGo}, indicating that evidence accumulation was slower for NoGo Decisions (Figure 6b). These modelling results provide a potential explanation on how local slow wave properties relate to mental states (Figure 4) and single-trial task performance (Figure 5). In other words, posterior slow waves were associated with sluggish responses and increased misses while frontal slow waves were associated with faster, impulsive responses and more false alarms. Indeed, slower evidence accumulation in favour of Go responses would lead to slower reaction times or even misses, whereas slower evidence accumulation for NoGo responses would lead to faster responses and possibly false alarms.

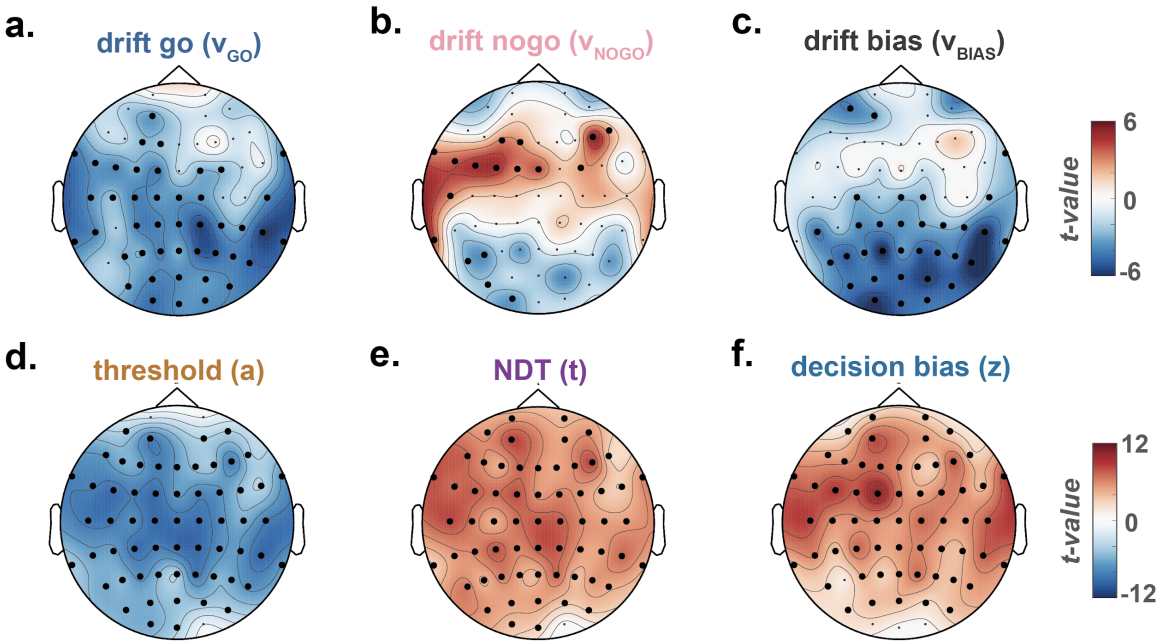

Figure 6. Global and local effects of the occurrence of slow waves on sub-components of decision-making

Reaction Times in the Go/NoGo tasks were modelled according to a Hierarchical Drift Diffusion Model (see Online Methods). a-f: Topographical maps of the effect of slow waves (i.e. whether or not a slow wave was detected for each trial and for a specific electrode) on the parameters of decision-making: drift Go [v_{Go}] (a), drift NoGo [v_{NoGo}] (b), drift bias [v_{Bias}] (c), threshold [a] (d), Non-decision time or NDT [t] (e), decision bias [z] (f). The effect of slow wave occurrence was estimated with LMEs (see Online

Methods) and topographies show the scalp distribution of the associated t-values. Black dots denote significant clusters of electrodes (pcluster<0.05, Bonferroni-corrected, see Online Methods).

These results suggest that slow waves could represent both a general index of fatigue as well as a mechanism underlying specific behavioural and subjective consequences of sleepiness. In other words, regardless of where it happens, slow waves can reflect the global "sleepiness" of an individual. Meanwhile, at a finer grain, depending on where they occur, slow waves can disrupt specific cognitive processes carried out by the affected brain regions. Taken together, we interpret this as strong evidence in support of the idea that slow waves are a compelling physiological phenomenon, which precedes and co-occurs with subjective and behavioural aspects of attentional lapses. In addition, our results indicate that spatio-temporal properties of slow waves can specifically explain distinctive components of behavioural and mental consequences of attentional lapses in a unified and quantitative manner.

Discussion

According to both in-lab and real-life studies, humans spend up to half of their waking lives not paying attention to their environment or any task at hand[34,35]. However, the ubiquitousness of these attentional lapses remains unexplained. Part of the difficulty in identifying their neural correlates could be due to their intrinsic diversity[7,8]. We embraced this challenge to clarify the neural mechanisms underlying attentional lapses by linking three different levels of explanation: behaviour, phenomenology and physiology. To grasp the phenomenological diversity of attentional lapses, we distinguish between MW and MB, where MW is operationally defined as a shift in attention away from environmental

416 demands and toward spontaneous task-unrelated thoughts, and MB as the absence of
417 thoughts and an empty mind. We propose that these two types of attentional lapses can be
418 explained by the occurrence of sleep-like low-frequency high-amplitude waves, where
419 regional differences in the occurrence of slow waves predicts the type of attentional lapse
420 as well as its behavioural profile. These slow waves have been previously linked to the
421 transition toward sleep when they are visible across the scalp[38] or to the concept of local
422 sleep when they occur in a subset of electrodes[11,22,25,29,30] and in the context of an awake
423 individual.

424 The concept of local sleep builds upon a recent questioning of the classical view of sleep
425 as an all-or-nothing phenomenon[22–24,41,42]. Although sleep is orchestrated at the scale of the
426 entire brain, some of the key neural mechanisms underlying sleep are implemented and
427 regulated at the level of local cortical circuits[24,25]. Consequently, when the pressure for
428 sleep increases, an awake brain can start displaying local sleep-like patterns of activity such
429 as delta or theta waves[21,22,29,43]. These bouts of local sleep-like activity, in the form of large-
430 amplitude slow waves, are both time-dependent (i.e. increase with time spent awake) and
431 use-dependent (i.e. depend on the level of activation of a given brain region)[29,30]. The
432 occurrence of slow waves has been linked to perturbations of information processing and
433 task-related errors or attentional lapses in animal and human intracranial data[21,22]. A similar
434 relationship between local sleep and behavioural errors has been evidenced when detecting
435 slow waves in non-invasive scalp recordings of sleep-deprived[29,30] or well-rested[31]
436 individuals.

437 Importantly, our study proposes a novel link between sleep-like slow waves in normal
438 wakefulness and both behaviour and subjective experience. Specifically, we showed that,

439 within the same individual, slow waves temporally precede different types of attentional
440 lapses. At the behavioural level, we observed that sluggish responses (slow responses and
441 misses) were associated with an increase in slow waves over posterior electrodes (Figure
442 5a,c). Conversely, impulsive responses (hasty responses and false alarms) were associated
443 with an increase in slow waves over frontal electrodes (Figure 5a-b). At the
444 phenomenological level, compared to task-focused (ON) reports, mind wandering (MW)
445 was preceded by an increase in slow-wave density, amplitude, upward and downward
446 slopes over frontal electrodes (Figure 4a). Compared to ON reports, mind blanking (MB)
447 was also preceded by an increase in slow-wave density over frontal electrodes, but we
448 additionally observed an increase in slow-wave upward and downward slopes over
449 posterior electrodes (Figure 4b). A direct comparison between MW and MB reports shows
450 that MB reports were associated with slow waves with steeper upward slopes over posterior
451 electrodes and smaller amplitude over frontal electrodes (Figure 4c). Finally, focusing on
452 shorter time windows (Figure S4-6), we showed that slow waves best predict mental states
453 (MW or MB vs ON) in the last few seconds before a probe, in line with previous
454 findings[44,45].

455 These results imply a spatial and temporal relationship between markers of local sleep and
456 behavioural errors: local sleep events, as measured through the presence of slow waves,
457 occurring at the right time (i.e. during stimulus presentation) and in the right place (i.e. in
458 the brain regions involved in the task) are predictive of distinct behavioural and
459 phenomenological aspects of attentional lapses[11].

460 Importantly, our results are largely consistent with previous findings on the neural
461 correlates of attentional lapses. Most of these studies focused on mind wandering, although

462 often defined as any mental state that is not on task (i.e. attentional lapses, which include
463 MW and MB as defined here). Early fMRI studies showed that mind wandering in this
464 sense was associated with the activation of the Default Mode Network (DMN)[46,47].
465 Relevant to our local sleep interpretation, the DMN is also suggested to be involved in
466 dream generation during sleep, consistent with the idea that the DMN supports a broad
467 array of experiences that are decoupled from the environment[48]. Furthermore, lesions
468 within the DMN are associated with a decrease in both mind wandering[49] and dreaming[50].
469 However, recent findings suggest a complex relationship between the DMN and
470 spontaneous experiences. Unlike what was initially hypothesized, the DMN is now
471 considered to be involved in both task-unrelated and task-related processes[44,51], depending
472 for example on environmental demands or the vividness of individuals' experiences[52,53].
473 Based on our results, we speculate that local sleep plays a key role in the complex
474 relationship between the DMN and spontaneous experiences. Previous studies have indeed
475 shown that a state of low alertness could induce the phasic activation of the DMN[54]. We
476 speculate that slow waves occurring within the DMN could lead to episodes of mind
477 wandering by disconnecting individuals from their environment[55]. Indeed, slow waves
478 during sleep have been proposed to be responsible for disconnecting sleepers from their
479 environment[27,56], as they are accompanied by a phenomenon of neuronal silencing that can
480 disrupt the processing of external inputs. If slow waves trigger specific occurrences of mind
481 wandering, other mechanisms could be responsible for the stability of these episodes[57].
482 Further investigations, including source localization or simultaneous recording of EEG and
483 fMRI[58,59], promise a deeper understanding of the mechanisms underlying these attentional
484 lapses.

485 Our work might also help reconcile previous findings on the EEG correlates of mind
486 wandering. A seminal study reported a reduction of alpha and/or beta oscillations during
487 mind wandering,[60] whereas others have reported an increase[61–63] . However, the relation
488 between alpha and sleep is complex: alpha power is low both when participants are fully
489 alert and, on the contrary, when approaching sleep onset[64,65]. Perhaps, the divergent results
490 obtained in previous studies regarding mind wandering and alpha oscillations could be
491 explained by different baseline levels of alpha oscillations in these studies. Likewise, past
492 pupilometry results on attentional lapses have been similarly inconclusive. While most
493 studies found a dampening of stimulus-locked increases in pupil size during mind
494 wandering (e.g. [47,66,67]), results diverge for baseline pupil size, which has been reported as
495 either increasing (e.g. [68,69]) or decreasing (e.g. [47,70,71]). When distinguished from mind
496 wandering, mind blanking has also been associated with reduced pupil size compared to
497 task-focused states[10,66]. Our results largely align with the latter results, with both mind
498 wandering and mind blanking being characterized by a decrease in pre-probe pupil size
499 (Figure 2e), which goes together with low vigilance ratings (Figure 2d) and an increase in
500 slow wave occurrence (Figure 3-4). In addition, the complex relations between pupil size
501 and mind wandering may be partly explained by the fact that pupil size does not index only
502 arousal but also correlates with motivation[72] and cognitive load[73], which also correlate with
503 mind wandering[2]. In contrast, the sleep-like nature of wake slow waves would make them
504 an unambiguous marker of sleepiness. Furthermore, slow waves are detected at the
505 electrode level and can therefore indicate how brain regions respond differently to sleep
506 pressure.

507 Other than mind wandering and blanking, we foresee that the spatio-temporal properties of

508 slow waves might predict other types of spontaneous experiences. For example, previous
509 research focusing on the hypnagogic period at sleep onset has shown that slow-wave like
510 activities are predictive of the occurrence of spontaneous imagery[74], the intensity of
511 thoughts[58] and can discriminate between different contents of spontaneous experiences[75].
512 Likewise, during sleep, it has been reported that local modulation of slow wave power is
513 predictive of the occurrence and contents of dreams[76]. Local sleep, therefore, might be
514 related to the type and content of spontaneous experiences not only during wakeful states,
515 as we showed here, but also during sleep-wake transitions and sleep.

516 Our results also speak to the broader question of how different brain regions participate in
517 shaping the stream of consciousness. Slow waves, considered as a perturbation of the
518 normal wake activity of local cortical networks, could reflect the functions of these
519 networks under normal situations. For example, we observed that slow waves in frontal
520 regions were associated with false alarms (Figure 5b), which aligns well with the role of
521 frontal cortices in executive functions and response inhibition[77]. Conversely, slow waves
522 in the back of the brain were associated with misses (Fig 5c), which is consistent with the
523 involvement of parietal cortices in sensorimotor integration[78]. At the phenomenological
524 level, frontal slow waves were associated with mind wandering, whereas posterior slow
525 waves were associated with mind blanking. Thus our results could speak to the debate on
526 the respective involvement of frontal and posterior cortices in supporting different
527 conscious states[79,80]. Our results suggest that a perturbation of frontal cortices leads to
528 unconstrained thoughts (mind wandering) rather than the loss of awareness, but that
529 awareness decreases when posterior regions momentarily go offline, a pattern similar to
530 the neural correlates of dreaming during sleep or spontaneous thoughts during wakeful

531 rest[58,76]. However, frontal and posterior slow waves do not only differ by their location but
532 also in terms of spatial expanse: slow waves in frontal electrodes appears more focal,
533 whereas slow waves in posterior electrodes is more widespread (Figure S10). Thus, the
534 loss of awareness during mind blanking could reflect a tendency for posterior slow waves
535 to involve a broader fronto-parietal network. This is in line with theories attributing an
536 essential role of fronto-parietal connections in the emergence of consciousness[81–83].

537 We speculate that the slow waves we report here are generated by similar neural
538 mechanisms as slow waves in sleep. Our speculation rests on the profile of slow waves
539 characterized in (i) time (Figure 3a) and (ii) space (Figure 3b,c), and the relationships
540 between slow wave properties and (iii) time spent on task (Figure S3), (iv) subjective
541 vigilance and (v) pupil size. While these five lines of evidence are correlational, we note
542 that together, they imply a high degree of similarity between slow waves in waking and
543 sleep. This, in turn, allows us to interpret wake slow waves as local sleep. Importantly, as
544 our study builds on convergent lines of indirect evidence to argue that the slow waves we
545 measured in waking participants are sleep-related, this interpretation is tentative and we do
546 not wish to suggest that the presence of slow-frequency oscillations in wake EEG is by
547 itself sufficient to establish a relation to sleep. Here, for example, we paired these
548 observations with objective (pupil size) and subjective (vigilance ratings) markers of
549 fatigue and checked that slow waves increased with the time spent on task. Future studies
550 could use direct evidence from intracranial recordings or sleep deprivation to more solidly
551 establish this interpretation. Intracranial recordings in particular can confirm whether wake
552 slow waves are accompanied by episodes of neuronal silencing, as for sleep slow waves,
553 and would help the identification of the exact neural mechanisms that generate the slow

554 waves we report here.

555 As our task involved the continuous presentation of visual stimuli, we could not fully
556 disentangle the occurrence of slow waves and task-related events. Yet, we showed that
557 slow waves differ from typical responses evoked by stimuli or participants' responses
558 (Figure S11). Future studies could include task-free resting state sessions to compare the
559 occurrence and properties of slow waves occurring during a task and without a task.
560 Relatedly, further investigation could help determine to which extent our findings
561 generalize to everyday situations (e.g., driving, attending a lecture, reading, etc).

562 It is worth noting that the tasks used here (SARTs) are rather undemanding and could
563 favour sleepiness and local sleep compared to more difficult and engaging experimental
564 paradigms. Generalising our findings to different experimental contexts or more
565 naturalistic settings would need further experimental validation[11]. From our findings, we
566 predict that slow waves would predict the occurrence of attentional lapses and mind
567 wandering in situations where participants feel rather sleepy and to a lesser extent or not at
568 all in situations where participants are well awake, motivated and highly engaged. We also
569 speculate that slow waves are not the only mechanism that underlies sensory decoupling in
570 wakefulness and sleep[56]. Other factors, such as the neuromodulation of brain activity, may
571 be critical in clarifying the total set of mechanisms underlying mind wandering[9,84] and
572 blanking, and more broadly attentional lapses.

573 In conclusion, we show here that attentional lapses occurring in the context of an
574 undemanding task are accompanied by sleep-like slow waves, even when participants are
575 well-rested. Furthermore, the location of slow waves is predictive of certain behavioural
576 and phenomenological properties of these lapses. Thus, we propose that these slow waves

577 reflect local intrusions of sleep within waking and constitute a mechanistic and proximate
578 cause to explain attentional lapses. Identifying a proximate mechanism of attentional lapses
579 could inspire novel applications leveraging brain-machine interfaces in educational or
580 professional settings.

581 Online Methods

582 ***Participants.*** Thirty-two (N=32) healthy adults were recruited and participated in this
583 study. Six individuals were not included in our analyses because of technical issues during
584 recordings or an abnormal quality of physiological recordings assessed through a post-hoc
585 visual inspection of the data. The remaining 26 participants (age: 29.8 ± 4.1 years, mean ±
586 standard-deviation; 10 females) were included in all analyses except for one individual for
587 whom we do not have eye-tracking data.

588 ***Experimental Design and Stimuli.*** Participants were seated in a dimly lit room with their
589 chin resting on a support at approximately 60cm from a computer screen. All task
590 instructions and stimuli were displayed and button responses were collected via the
591 Psychtoolbox extension[85] for Matlab (Mathworks, Natick, MA, USA).

592 The experimental design consisted of two modified Sustained Attention to Response Tasks
593 (SARTs)[32] in which participants were instructed to pay attention to a series of pictures of
594 human faces in the Face SART blocks or digits in the Digit SART blocks. The order of
595 Face or Digit blocks was pseudo-randomized for each participant. Each block lasted
596 approximately 12 to 15 minutes. Participants were allowed to rest between blocks.
597 Participants performed 3 Face SART blocks and 3 Digit SART blocks for a total duration
598 of 103 ± 19.7 minutes (mean ± standard-deviation) from beginning to end. Each type of

599 the Face and Digit SART was preceded by a brief training session (27 trials) on each SART.
600 During this SART training session, feedback on the proportion of correct trials and average
601 reaction times was provided to participants. Participants were encouraged to prioritize
602 accuracy over speed.

603 Face and digit stimuli were presented continuously, each stimulus appearing for a duration
604 of 750 to 1250ms (random uniform jitter). Face stimuli were extracted from the Radboud
605 Face Database[86] and consisted of 8 faces (4 females) with a neutral facial expression and
606 one smiling female face. Digits from 1 to 9 were displayed with a fixed font size. For the
607 Face SART, participants were instructed to press a button for all neutral faces (Go trials)
608 but to avoid pressing the response button for the smiling face (NoGo trials). The order of
609 faces was pseudo-randomized throughout the entire task (i.e. we permuted the presentation
610 order every 9 stimuli and we did not present twice the same stimuli in a row). For the Digit
611 SART, participants were instructed to press a button for all digits except the digit "3"
612 (NoGo trials), with the order of the digits pseudo-randomized as well.

613 During the SART, we stopped the presentation of stimuli at random times (every 30 to 70s,
614 random uniform jitter) with a sound and the word "STOP" displayed on the screen. These
615 interruptions allowed us to probe the mental state of the participants with a series of 8
616 questions (including 1 conditional question; see Supplementary Methods). In particular,
617 we instructed participants to report their attentional focus "just before the interruption".
618 Participants had to select one of the four following options: (1) "task-focused" (i.e.
619 focusing on the task, ON), (2) "off-task" (i.e. focusing on something other than the task,
620 which we define here as mind wandering MW), (3) "mind blanking" (i.e. focusing on
621 nothing), (4) "don't remember". As the 4th option accounted for only 1.1% of all probes

622 (i.e. less than 1 probe per participant on average) and since previous studies do not always
623 distinguish between these options (e.g. [87]), we collapsed the 3rd and 4th options as mind-
624 blanking (MB) in all analyses. We also instructed participants to rate their level of
625 vigilance, reflecting "over the past few trials", with a 4-point scale (Figure 2d; from
626 1="Extremely Sleepy" to 4="Extremely Alert"). Each of the 12-15 min SART blocks
627 included 10 interruptions (in total, 30 interruptions for each SART task and 60 interruptions
628 per participant). Participants were informed of the presence of interruptions and the nature
629 of each question before starting the experiment. The mental state categories (ON, MW and
630 MB) were also explained to participants orally and in writing.

631 ***Physiological Recordings and Preprocessing.*** High-density scalp electroencephalography
632 (EEG) was recorded using an EasyCap (63 active electrodes) connected to a BrainAmp
633 system (Brain Products GmbH). A ground electrode was placed frontally (Fpz in the 10-
634 20 system). Electrodes were referenced online to a frontal electrode (AFz). Additional
635 electrodes were placed above and below the left and right canthi respectively to record
636 ocular movements (electrooculogram, EOG). Two electrodes were placed over the deltoid
637 muscles to record electrocardiographic (ECG) activity. EEG, EOG and ECG were sampled
638 at 500Hz. Eye-movements and pupil size on one eye were recorded with an EyeLink 1000
639 system (SR Research) with a sampling frequency of 1000Hz. The eye-tracker was
640 calibrated at the start of each recording using the EyeLink acquisition software.

641 The EEG signal was analysed in Matlab with a combination of the SPM12, EEGlab[88] and
642 Fieldtrip[89] toolboxes. The raw EEG signal was first high-pass filtered above 0.1 Hz using
643 a two-pass 5th-order Butterworth filter. A notch filter was then applied (stop-band: [45, 55]
644 Hz, 4th-order Butterworth filter) to remove line noise. Electrodes that were visually

645 identified as noisy throughout the recording were removed and interpolated using
646 neighbouring electrodes. Finally, the continuous EEG data was segmented according to
647 probe onsets on a 64s window ([-32, 32] s relative to the probe onset); the average voltage
648 over the entire window (64s) was then removed for each electrode and probe.

649 Pupil size was analysed with custom functions in Matlab and corrected for the occurrence
650 of blinks (see [33] and Supplementary Methods). Pupil size was averaged over the stimulus
651 presentation window for each trial (window length: 0.75 to 1.25s). Pupil size values in
652 Figure 2e were computed by averaging the pupil size in all trials within 20s preceding the
653 probe onset and then by discretizing them into 5 bins across all probes for each participant
654 and task, to normalize pupil size across participants[33].

655 ***Behavioural Analyses.*** Go trials were considered incorrect (Miss) if no response was
656 recorded between stimulus onset and the next stimulus onset. Conversely, NoGo trials were
657 considered incorrect (false alarm) if a response was recorded between stimulus onset and
658 the next stimulus onset. Reaction times were computed from the onset of the stimulus
659 presentation. Trials with reaction times shorter than 300ms were excluded from all analyses
660 (so not considered correct or incorrect). In all subsequent analyses, we focused only on
661 trials within 20s from probe onset. The choice of a 20s-window allowed the inclusion of 2
662 NoGo trials for each probe, while focusing on trials that are relatively close to the probe
663 onset and subsequent subjective reports. Since previous studies sometimes examined
664 shorter pre-probe time windows (e.g. [44]), we also analysed the data with shorter time
665 windows (Table S3 and Figure S4-6).

666 ***Detection of Slow Waves.*** The detection of sleep-like slow waves in waking was based on
667 previous algorithms devised to automatically detect slow waves during NREM sleep[30,37].

668 First, the preprocessed EEG signal was re-referenced to the average of the left and right
669 mastoid electrodes (TP9 and TP10) to match the established guidelines for sleep
670 recordings[90]. Then, the signal was down-sampled to 128Hz and band-pass filtered within
671 the delta band. A type-2 Chebyshev filter was used to reach an attenuation of at least 25
672 dB in the stop-band ([0.1, 15] Hz) but less than 3 dB in the pass-band ([1, 10] Hz). All
673 waves were detected by locating the negative peaks in the filtered signal. For each wave,
674 the following parameters were extracted: start and end point (defined as zero-crossing
675 respectively prior the negative peak of the wave and following its positive peak), negative
676 peak amplitude and position in time, positive peak amplitude and position in time, peak-
677 to-peak amplitude, downward (from start to negative peak) and upward (from negative to
678 positive peak) slopes.

679 Slow waves in sleep typically have a larger negative peak compared to their positive peak
680 (Figure 3a) and are predominantly observed over fronto-central channels[37,38] (Figure 3b).
681 This contrasts with artefacts in the EEG signal caused by blinks, which typically have a
682 large positive component and are more frontally distributed. To reduce the false detection
683 of these artefacts as candidate slow waves, we excluded waves with a positive peak above
684 75µV. We also excluded waves within 1s of large-amplitude events (>150µV of absolute
685 amplitude). Finally, we discarded all waves that were shorter than 143ms in duration
686 (corresponding to a frequency > 7Hz). We then selected the waves with the highest
687 absolute peak-to-peak amplitude (top 10% computed for each electrode independently) as
688 local sleep slow waves. This 10% threshold was selected based on the visual examination
689 of the distribution of the amplitudes at the subject level (see Figure S12 for the
690 corresponding topography). The mean ± SEM of the threshold voltage across subjects was

691 30.7 ± 1.5 μV. Finally, we compared slow waves with neural activity related to task events
692 (stimulus onsets and motor responses). To do so, we computed the event related potentials
693 (ERPs) by averaging, across participants, the EEG signal band passed around 0.1 and 30Hz
694 and referenced to the mastoids. These ERPs were locked either on slow-waves' start,
695 stimulus onset (for face and digit stimuli separately) or motor responses. The corresponding
696 temporal profiles are shown in Figure S11a-c for electrode Cz.

697 ***Hierarchical Drift Diffusion Modelling***. Hierarchical Bayesian Drift Diffusion Modelling
698 (HDDM) was used to extend our analysis beyond simple behavioural metrics and examine
699 the impact of mental states (Figure S9) and slow waves (Figure 6) on the sub-processes of
700 decision making. The DDM is a sequential-sampling model of 2AFC decision making that
701 can be considered an extension of signal detection theory into the time-domain, accounting
702 for full reaction time distributions as well as choice behaviour[39]. The HDDM package[40] in
703 Python 2.8 was used to fit the drift-diffusion model to the SART data. DDM parameters
704 were estimated using a hierarchical Bayesian method that uses Markov-chain Monte Carlo
705 (MCMC) sampling to generate full posterior distributions of model parameters. The
706 following DDM parameters were estimated: the drift rate for Go trials (v_{Go}), the drift rate
707 for NoGo trials (v_{NoGo}), the decision threshold (a), the decision bias (z) and the non-decision
708 time (t). Drift bias (v_{Bias}) was computed by taking the difference between the absolute
709 values of v_{Go} (positive) and v_{NoGo} (negative), where greater values indicate stronger v_{Go}
710 drift bias (Figure S7). To examine whether the model could reproduce key patterns in the
711 SART data, posterior predictive checks were undertaken by simulating 100 datasets from
712 the joint posteriors of model parameters and comparing these to the observed data[91] (Figure
713 S8).

To estimate HDDM parameters 8,000 samples from the posterior were generated with MCMC methods and the initial 2,000 were discarded as burn-in to reduce autocorrelation. HDDM models were first fit on the trials preceding subjective reports to examine the influence of mental states on decision parameters (Figure S9). HDDM parameters were free to vary by state and task. From the estimated models, we extracted the subject-level point-estimates of parameters as the mean of each individual's posterior distribution for a given task (Face and Digit) and mental state (ON, MW or MB). We then fitted HDDM models so as to examine the influence of slow waves (event present vs. absent; Figure 6). To do so we considered each EEG electrode separately. For a given electrode, a trial was flagged as being associated with slow waves if the onset of a slow wave was detected for this electrode during stimulus presentation (i.e. between stimulus onset and offset). Parameters were also free to vary by task (Digit vs. Face). When examining the impact of mental states or slow waves on HDDM parameters, we included trials within 20s of a probe onset (allowing to include 2 NoGo trials for each probe). From the estimated models, we extracted the subject-level point-estimates of parameters as the mean of each individual's posterior distribution for a given task (Face and Digit) and slow waves (present or absent). Statistical comparisons were performed on the subject-level point-estimates.

Statistical Analyses. Statistics were performed using Linear Mixed-Effects modelling (LMEs). In all models, subject identity was coded as a categorical random effect. The task type (Digit or Face SART) was used as a categorical fixed effect in all analyses. Several fixed effects were independently tested in our different analyses: mental state (categorical variable: ON, MW and MB; Figure 2-4) or slow waves (binary variable: present/absent, Figure 5). LMEs were run to predict different variables of interest: behavioural variables

737 (misses, false alarms, reaction times) or physiological variables (pupil size, presence or
738 properties of slow waves). We also used LMEs to estimate the effect of mental states or
739 slow waves on the point-estimates derived from the HDDM models (Figure S9 and Figure
740 6). Model comparisons were performed using a Likelihood Ratio Test to estimate the
741 influence of multi-level categorical variables such as mental states. In practice, we
742 compared a model including mental state (along possibly other random and fixed effects)
743 with a model not including mental state as a predictor. All models and model comparisons
744 are described in Supplementary Table 1. In the Results section, we report the Likelihood
745 Ratio Test as χ^2(df), where χ^2 is the Likelihood Ratio Test statistic and df the degrees of
746 freedom[92,93]. When several model comparisons were performed for the same analysis using
747 the Likelihood Ratio Test, a Bonferroni correction was applied to the statistical threshold.
748 To indicate the magnitude and direction of the effects, we report the estimates (β) and
749 confidence interval (CI) for the contrasts of interest (MW vs. ON, MB vs ON, MB vs MW).
750 All models performed are described in Supplementary Table 1. For topographical maps,
751 clusters were identified using a cluster-permutation approach. In practice, for each
752 electrode, we extracted the t-values and p-values for the effects of interest. Clusters of
753 neighbouring electrodes were defined as electrodes with p-values below 0.025 (cluster
754 alpha). Once the clusters were defined, a comparison was performed with permuted
755 datasets and we used a Monte-Carlo p-value threshold of 0.05 to identify the significant
756 clusters ($p_{cluster}$, see Supplementary Methods for details). This threshold was corrected for
757 multiple comparisons when several non-independent cluster permutations were performed
758 (e.g. Figure 4-6, S2-4) in order to keep the type-1 error rate constant across analyses.

Acknowledgments

TA and NT were supported by Australian Research Council Discovery Projects (DP180104128 and DP180100396) and National Health Medical Research Council Ideas Projects (APP1183280). TA was supported by a Long-Term Fellowship from the Human Frontier Science Program (LT000362/2018-L). JW was supported by Australian Research Council Discovery Early Career Researcher Awards (DE170101254). We thank Devangna Tangri for her help in data collection and Giulio Bernardi for sharing his slow-wave detection algorithm. We also thank our reviewers, Dr Tristan Bekeinschtein, Dr Jonathan Smallwood and a third anonymous reviewer for their constructive comments and criticisms.

Author Contributions

Design: TA, TM, JW & NT. Data collection: TA & TM. Analyses: TA & AB.

Manuscript: TA, AB, JW & NT.

Data Availability

All raw data and code generated for this study are publicly available:

Raw data: https://osf.io/ey3ca/?view_only=680c39e7065649c3b783a4efec0a1a94
Code used for analyses: https://github.com/andrillon/wanderIM

References

1. Chun, M. M., Golomb, J. D. & Turk-Browne, N. B. A Taxonomy of External and Internal Attention. *Annual Review of Psychology* **62**, 73–101 (2011).
2. Smallwood, J. & Schooler, J. W. The Science of Mind Wandering: Empirically Navigating the Stream of Consciousness. *Annual Review of Psychology* **66**, 487–518 (2015).
3. Ward, A. F. & Wegner, D. M. Mind-blanking: when the mind goes away. *Frontiers in Psychology* **4**, (2013).
4. Seli, P., Risko, E. F., Smilek, D. & Schacter, D. L. Mind-Wandering With and Without Intention. *Trends in Cognitive Sciences* **20**, 605–617 (2016).
5. VanRullen, R. Perceptual Cycles. *Trends in Cognitive Sciences* **20**, 723–735 (2016).
6. Johnson, K. A. *et al.* Response variability in Attention Deficit Hyperactivity Disorder: Evidence for neuropsychological heterogeneity. *Neuropsychologia* **45**, 630–638 (2007).
7. Seli, P. *et al.* Mind-Wandering as a Natural Kind: A Family-Resemblances View. *Trends in Cognitive Sciences* **22**, 479–490 (2018).
8. Christoff, K. *et al.* Mind-Wandering as a Scientific Concept: Cutting through the Definitional Haze. *Trends Cogn. Sci. (Regul. Ed.)* **22**, 957–959 (2018).
9. Mittner, M., Hawkins, G. E., Boekel, W. & Forstmann, B. U. A Neural Model of Mind Wandering. *Trends in Cognitive Sciences* **20**, 570–578 (2016).
10. Unsworth, N. & Robison, M. K. Tracking arousal state and mind wandering with pupillometry. *Cognitive, Affective, & Behavioral Neuroscience* **18**, 638–664 (2018).

802 11. Andrillon, T. *et al.* Does the Mind Wander When the Brain Takes a Break? Local
803 Sleep in Wakefulness, Attentional Lapses and Mind-Wandering. *Frontiers in*
804 *Neuroscience* **13**, (2019).
805 12. Drummond, S. P. A., Paulus, M. P. & Tapert, S. F. Effects of two nights sleep
806 deprivation and two nights recovery sleep on response inhibition. *Journal of Sleep*
807 *Research* **15**, 261–265 (2006).
808 13. Doran, S. M., Van Dongen, H. P. & Dinges, D. F. Sustained attention performance
809 during sleep deprivation: evidence of state instability. *Arch Ital Biol* **139**, 253–267
810 (2001).
811 14. Metin, B. *et al.* ADHD performance reflects inefficient but not impulsive information
812 processing: A diffusion model analysis. *Neuropsychology* **27**, 193–200 (2013).
813 15. Poh, J.-H., Chong, P. L. H. & Chee, M. W. L. Sleepless night, restless mind: Effects
814 of sleep deprivation on mind wandering. *Journal of Experimental Psychology:*
815 *General* **145**, 1312–1318 (2016).
816 16. Madiouni, C., Lopez, R., Gély-Nargeot, M.-C., Lebrun, C. & Bayard, S. Mind-
817 wandering and sleepiness in adults with attention-deficit/hyperactivity disorder.
818 *Psychiatry Research* **287**, 112901 (2020).
819 17. Goupil, L. & Bekinschtein, T. A. Cognitive processing during the transition to sleep.
820 *Arch Ital Biol* **150**, 140–154 (2012).
821 18. Nielsen, T. Microdream neurophenomenology. *Neuroscience of Consciousness* **2017**,
822 (2017).
823 19. Cirelli, C. & Tononi, G. Is sleep essential? *PLoS Biol.* **6**, e216 (2008).

824 20. Tononi, G. & Cirelli, C. Sleep and the Price of Plasticity: From Synaptic and Cellular
825 Homeostasis to Memory Consolidation and Integration. *Neuron* **81**, 12–34 (2014).
826 21. Nir, Y. *et al.* Selective neuronal lapses precede human cognitive lapses following
827 sleep deprivation. *Nature Medicine* **23**, 1474–1480 (2017).
828 22. Vyazovskiy, V. V. *et al.* Local sleep in awake rats. *Nature* **472**, 443–7 (2011).
829 23. Krueger, J. M., Nguyen, J. T., Dykstra-Aiello, C. J. & Taishi, P. Local sleep. *Sleep*
830 *Medicine Reviews* **43**, 14–21 (2019).
831 24. Rector, D. M., Schei, J. L., Van Dongen, H. P. A., Belenky, G. & Krueger, J. M.
832 Physiological markers of local sleep. *European Journal of Neuroscience* **29**, 1771–
833 1778 (2009).
834 25. D'Ambrosio, S. *et al.* Sleepiness as a Local Phenomenon. *Frontiers in Neuroscience*
835 **13**, (2019).
836 26. Steriade, M. *Neuronal Substrates of Sleep and Epilepsy*. vol. 1 (Cambridge
837 University Press, 2003).
838 27. Tononi, G. & Massimini, M. Why does consciousness fade in early sleep? *Ann. N. Y.*
839 *Acad. Sci.* **1129**, 330–334 (2008).
840 28. Andrillon, T., Poulsen, A. T., Hansen, L. K., Leger, D. & Kouider, S. Neural Markers
841 of Responsiveness to the Environment in Human Sleep. *Journal of Neuroscience* **36**,
842 6583–6596 (2016).
843 29. Hung, C.-S. *et al.* Local experience-dependent changes in the wake EEG after
844 prolonged wakefulness. *Sleep* **36**, 59–72 (2013).

30. Bernardi, G. *et al.* Neural and Behavioral Correlates of Extended Training during Sleep Deprivation in Humans: Evidence for Local, Task-Specific Effects. *Journal of Neuroscience* **35**, 4487–4500 (2015).

31. Quercia, A., Zappasodi, F., Committeri, G. & Ferrara, M. Local Use-Dependent Sleep in Wakefulness Links Performance Errors to Learning. *Frontiers in Human Neuroscience* **12**, (2018).

32. Robertson, I. H., Manly, T., Andrade, J., Baddeley, B. T. & Yiend, J. 'Oops!': performance correlates of everyday attentional failures in traumatic brain injured and normal subjects. *Neuropsychologia* **35**, 747–758 (1997).

33. van Kempen, J. *et al.* Behavioural and neural signatures of perceptual decision-making are modulated by pupil-linked arousal. *eLife* **8**, (2019).

34. Killingsworth, M. A. & Gilbert, D. T. A Wandering Mind Is an Unhappy Mind. *Science* **330**, 932–932 (2010).

35. Seli, P., Carriere, J. S. A., Levene, M. & Smilek, D. How few and far between? Examining the effects of probe rate on self-reported mind wandering. *Frontiers in Psychology* **4**, (2013).

36. Joshi, S., Li, Y., Kalwani, R. M. & Gold, J. I. Relationships between Pupil Diameter and Neuronal Activity in the Locus Coeruleus, Colliculi, and Cingulate Cortex. *Neuron* **89**, 221–234 (2016).

37. Riedner, B. A. *et al.* Sleep homeostasis and cortical synchronization: III. A high-density EEG study of sleep slow waves in humans. *Sleep* **30**, 1643–57 (2007).

38. Siclari, F. *et al.* Two Distinct Synchronization Processes in the Transition to Sleep: A High-Density Electroencephalographic Study. *SLEEP* (2014) doi:10.5665/sleep.4070.

39. Ratcliff, R., Smith, P. L., Brown, S. D. & McKoon, G. Diffusion Decision Model: Current Issues and History. *Trends in Cognitive Sciences* **20**, 260–281 (2016).

40. Wiecki, T. V., Sofer, I. & Frank, M. J. HDDM: Hierarchical Bayesian estimation of the Drift-Diffusion Model in Python. *Frontiers in Neuroinformatics* **7**, (2013).

41. Nir, Y. *et al.* Regional slow waves and spindles in human sleep. *Neuron* **70**, 153–69 (2011).

42. Siclari, F. & Tononi, G. Local aspects of sleep and wakefulness. *Current Opinion in Neurobiology* **44**, 222–227 (2017).

43. Rector, D. M., Topchiy, I. A., Carter, K. M. & Rojas, M. J. Local functional state differences between rat cortical columns. *Brain Research* **1047**, 45–55 (2005).

44. Sormaz, M. *et al.* Default mode network can support the level of detail in experience during active task states. *Proceedings of the National Academy of Sciences* **115**, 9318–9323 (2018).

45. Ellamil, M. *et al.* Dynamics of neural recruitment surrounding the spontaneous arising of thoughts in experienced mindfulness practitioners. *NeuroImage* **136**, 186–196 (2016).

46. Mason, M. F. *et al.* Wandering minds: the default network and stimulus-independent thought. *Science* **315**, 393–5 (2007).

47. Mittner, M. *et al.* When the Brain Takes a Break: A Model-Based Analysis of Mind Wandering. *The Journal of Neuroscience* **34**, 16286–16295 (2014).

48. Fox, K. C. R., Nijeboer, S., Solomonova, E., Domhoff, G. W. & Christoff, K. Dreaming as mind wandering: evidence from functional neuroimaging and first-person content reports. *Frontiers in Human Neuroscience* **7**, (2013).
49. Philippi, C. L. *et al.* Lesion network mapping demonstrates that mind-wandering is associated with the default mode network. *J Neurosci Res* **99**, 361–373 (2021).
50. Zellner, M. R. Dreaming and the Default Mode Network: Some Psychoanalytic Notes. *Contemporary Psychoanalysis* **49**, 226–232 (2013).
51. Konu, D. *et al.* A role for the ventromedial prefrontal cortex in self-generated episodic social cognition. *NeuroImage* **218**, 116977 (2020).
52. Turnbull, A. *et al.* Left dorsolateral prefrontal cortex supports context-dependent prioritisation of off-task thought. *Nature Communications* **10**, (2019).
53. Turnbull, A. *et al.* The ebb and flow of attention: Between-subject variation in intrinsic connectivity and cognition associated with the dynamics of ongoing experience. *NeuroImage* **185**, 286–299 (2019).
54. Tagliazucchi, E. & Laufs, H. Decoding Wakefulness Levels from Typical fMRI Resting-State Data Reveals Reliable Drifts between Wakefulness and Sleep. *Neuron* **82**, 695–708 (2014).
55. Kam, J. W. Y. *et al.* Slow Fluctuations in Attentional Control of Sensory Cortex. *Journal of Cognitive Neuroscience* **23**, 460–470 (2011).
56. Andrillon, T. & Kouider, S. The vigilant sleeper: neural mechanisms of sensory (de)coupling during sleep. *Current Opinion in Physiology* (2019) doi:10.1016/j.cophys.2019.12.002.

57. Smallwood, J. Distinguishing how from why the mind wanders: A process–occurrence framework for self-generated mental activity. *Psychological Bulletin* **139**, 519–535 (2013).

58. Perogamvros, L. *et al.* The Phenomenal Contents and Neural Correlates of Spontaneous Thoughts across Wakefulness, NREM Sleep, and REM Sleep. *Journal of Cognitive Neuroscience* 1–12 (2017) doi:10.1162/jocn_a_01155.

59. Hawes, S. *et al. Sleeping While Awake: The Intrusion of Neural Activity Associated with Sleep Onset in the Awake Human Brain*. http://biorxiv.org/lookup/doi/10.1101/2020.06.04.133603 (2020) doi:10.1101/2020.06.04.133603.

60. Braboszcz, C. & Delorme, A. Lost in thoughts: Neural markers of low alertness during mind wandering. *NeuroImage* **54**, 3040–3047 (2011).

61. Compton, R. J., Gearinger, D. & Wild, H. The wandering mind oscillates: EEG alpha power is enhanced during moments of mind-wandering. *Cognitive, Affective, & Behavioral Neuroscience* **19**, 1184–1191 (2019).

62. Macdonald, J. S. P., Mathan, S. & Yeung, N. Trial-by-Trial Variations in Subjective Attentional State are Reflected in Ongoing Prestimulus EEG Alpha Oscillations. *Frontiers in Psychology* **2**, (2011).

63. Arnau, S. *et al.* Inter-trial alpha power indicates mind wandering. *Psychophysiology* **57**, (2020).

64. Hori, T., Hayashi, M. & Morikawa, T. Topographical EEG changes and the hypnagogic experience. in *Sleep onset: Normal and abnormal processes.* (eds. Ogilvie, R. D. & Harsh, J. R.) 237–253 (American Psychological Association, 1994).

65. Jagannathan, S. R. *et al.* Tracking wakefulness as it fades: Micro-measures of alertness. *NeuroImage* **176**, 138–151 (2018).

66. Unsworth, N. & Robison, M. K. Pupillary correlates of lapses of sustained attention. *Cognitive, Affective, & Behavioral Neuroscience* **16**, 601–615 (2016).

67. Smallwood, J. *et al.* Pupillometric Evidence for the Decoupling of Attention from Perceptual Input during Offline Thought. *PLoS ONE* **6**, e18298 (2011).

68. Smallwood, J. *et al.* Insulation for Daydreams: A Role for Tonic Norepinephrine in the Facilitation of Internally Guided Thought. *PLoS ONE* **7**, e33706 (2012).

69. Franklin, M. S., Broadway, J. M., Mrazek, M. D., Smallwood, J. & Schooler, J. W. Window to the Wandering Mind: Pupillometry of Spontaneous Thought While Reading. *Quarterly Journal of Experimental Psychology* **66**, 2289–2294 (2013).

70. Grandchamp, R., Braboszcz, C. & Delorme, A. Oculometric variations during mind wandering. *Frontiers in Psychology* **5**, (2014).

71. Konishi, M., Brown, K., Battaglini, L. & Smallwood, J. When attention wanders: Pupillometric signatures of fluctuations in external attention. *Cognition* **168**, 16–26 (2017).

72. Varazzani, C., San-Galli, A., Gilardeau, S. & Bouret, S. Noradrenaline and Dopamine Neurons in the Reward/Effort Trade-Off: A Direct Electrophysiological Comparison in Behaving Monkeys. *Journal of Neuroscience* **35**, 7866–7877 (2015).

73. Kahneman, D. & Beatty, J. Pupil Diameter and Load on Memory. *Science* **154**, 1583–1585 (1966).

74. Germain, A. & Nielsen, T. A. EEG power associated with early sleep onset images differing in sensory content. *Sleep Research Online* **4**, 83–90 (2001).

75. Noreika, V. *et al.* Intrusions of a drowsy mind: neural markers of phenomenological unpredictability. *Frontiers in Psychology* **6**, (2015).

76. Siclari, F. *et al.* The neural correlates of dreaming. *Nature Neuroscience* **20**, 872–878 (2017).

77. Simmonds, D. J., Pekar, J. J. & Mostofsky, S. H. Meta-analysis of Go/No-go tasks demonstrating that fMRI activation associated with response inhibition is task-dependent. *Neuropsychologia* **46**, 224–232 (2008).

78. Lynch, J. C. The functional organization of posterior parietal association cortex. *Behavioral and Brain Sciences* **3**, 485–499 (1980).

79. Boly, M. *et al.* Are the Neural Correlates of Consciousness in the Front or in the Back of the Cerebral Cortex? Clinical and Neuroimaging Evidence. *J. Neurosci.* **37**, 9603–9613 (2017).

80. Odegaard, B., Knight, R. T. & Lau, H. Should a Few Null Findings Falsify Prefrontal Theories of Conscious Perception? *The Journal of Neuroscience* **37**, 9593–9602 (2017).

81. Dehaene, S., Changeux, J.-P., Naccache, L., Sackur, J. & Sergent, C. Conscious, preconscious, and subliminal processing: a testable taxonomy. *Trends in Cognitive Sciences* **10**, 204–211 (2006).

82. Mashour, G. A., Roelfsema, P., Changeux, J.-P. & Dehaene, S. Conscious Processing and the Global Neuronal Workspace Hypothesis. *Neuron* **105**, 776–798 (2020).

83. Dehaene, S., Kerszberg, M. & Changeux, J. P. A neuronal model of a global workspace in effortful cognitive tasks. *Proc Natl Acad Sci U S A* **95**, 14529–34 (1998).

980 84. O'Callaghan, C., Walpola, I. C. & Shine, J. M. Neuromodulation of the mind-
981 wandering brain state: the interaction between neuromodulatory tone, sharp wave-
982 ripples and spontaneous thought. *Phil. Trans. R. Soc. B* **376**, 20190699 (2021).
983 85. Brainard, D. H. The Psychophysics Toolbox. *Spat Vis* **10**, 433–436 (1997).
984 86. Langner, O. *et al.* Presentation and validation of the Radboud Faces Database.
985 *Cognition & Emotion* **24**, 1377–1388 (2010).
986 87. Van den Driessche, C. *et al.* Attentional Lapses in Attention-Deficit/Hyperactivity
987 Disorder: Blank Rather Than Wandering Thoughts. *Psychological Science* **28**, 1375–
988 1386 (2017).
989 88. Delorme, A. & Makeig, S. EEGLAB: an open source toolbox for analysis of single-
990 trial EEG dynamics including independent component analysis. *J. Neurosci. Methods*
991 **134**, 9–21 (2004).
992 89. Oostenveld, R., Fries, P., Maris, E. & Schoffelen, J.-M. FieldTrip: Open source
993 software for advanced analysis of MEG, EEG, and invasive electrophysiological
994 data. *Comput Intell Neurosci* **2011**, 156869 (2011).
995 90. Iber, C., Ancoli-Israel, S., Chesson, A. & Quan, S. The AASM Manual for the
996 Scoring of Sleep and Associated Events: Rules, Terminology and Technical
997 Specifications. (2007).
998 91. Gelman, A., Meng, X.-L. & Stern, H. Posterior predictive assessment of model
999 fitness via realized discrepancies. *Statistica sinica* 733–760 (1996).
1000 92. Bates, D., Mächler, M., Bolker, B. & Walker, S. Fitting Linear Mixed-Effects Models
1001 Using **lme4**. *Journal of Statistical Software* **67**, (2015).

1002 93. Harrison, X. A. *et al.* A brief introduction to mixed effects modelling and multi-
1003 model inference in ecology. *PeerJ* **6**, e4794 (2018).
1004

Supplementary Information:

Predicting lapses of attention with sleep-like slow waves.

Thomas Andrillon[1]*, Angus Burns[1], Teigane MacKay[1], Jennifer Windt[2] & Naotsugu Tsuchiya[1,3,4]

Affiliations:

1. School of Psychological Sciences, Turner Institute for Brain and Mental Health, Monash University, Melbourne 3168, Victoria, Australia.
2. Philosophy Department, Monash University, Melbourne 3168, Victoria, Australia.
3. Center for Information and Neural Networks (CiNet), National Institute of Information and Communications Technology (NICT), Suita, Osaka 565-0871, Japan
4. Advanced Telecommunications Research Computational Neuroscience Laboratories, 2-2-2 Hikaridai, Seika-cho, Soraku-gun, Kyoto 619-0288, Japan.

Supplementary Methods

Supplementary Table 1 to 3

Supplementary Figures 1 to 12

Supplementary Methods

Participants. Prior to their participation in the protocol, all 26 participants but one filled in online surveys on Qualtrics (N=25). They reported normal levels of sleepiness (Epworth Sleepiness Scale: 14.6 ± 4.7; mean ± standard-deviation) and mind wandering (Mind Wandering Questionnaire[1]: 3.6 ± 0.91) in their everyday lives. Participants were not instructed to follow a particular schedule before the experiment (in particular, our protocol did not involve a sleep restriction procedure). The timing of the experiment was determined by participants' availability and included both morning and afternoon sessions.

Experimental Design and Stimuli. Face stimuli were divided in two parts vertically (half-left and half-right faces) which were flickered on the screen at different frequencies (12 and 15 Hz, counterbalanced across participants). Similarly, the digits were inserted in a Kanizsa illusory square (Fig. 1a) whose right and left parts also flickered at different frequencies (12 and 15 Hz). This flickering was introduced to elicit Steady State Visual Evoked Potentials (SSVEPs) in the EEG signal. The detailed analysis of this aspect of our dataset will be reported elsewhere. As the flickering occurred at a high rate, participants did not report a negative effect on their ability to perform the SART.

Experience Sampling. Following task interruptions (probes), participants were asked to answer a series of 8 questions in the following fixed order: (1) 'Were you looking at the screen?' (response: yes / no); (2) 'Where was your attention focus?' (response: on-task / off-task / blank / don't remember); (3) 'What distracted your attention from the task?' (response: Something in the room / personal / about the task); (4) 'How aware were you of your focus?' (response: from 1, I was fully aware, to 4, I was not aware at all); (5) 'Was your state of mind intentional?' (response: from 1, entirely intentional, to 4, entirely unintentional); (6) 'How engaging were your thoughts?' (response: from 1, not engaging, to 4, very engaging); (7) 'How well do you

think you have been performing?' (response: from 1, not good, to 4, very good); (8) 'How alert have you been?' (response: extremely alert / alert / sleepy / extremely sleepy). Question 3 was displayed only if participants answered off-task in question 1. In this report, we focus only on questions (2) and (8).

Physiological Recordings and Preprocessing. The raw pupil size was corrected for the occurrence of blinks as in[2]. The timings of blinks were obtained through the EyeLink acquisition software. For each of these blinks, the pupil size was corrected by linearly interpolating the average signal preceding the blink onset ([-0.2, -0.1]s) and following the blink offset ([0.1, 0.2]s). The corrected signal was then low-pass filtered below 6Hz (two-pass Butterworth filter at the 4th order). Finally, for blinks longer than 2s, data points between -0.1s prior to blink onset and 0.1s after blink onset were considered missing.

Detection of Slow Waves. In sleep, according to established guidelines[3], only waves with peak-to-peak amplitude exceeding 75µV are defined as slow waves. In wakefulness, similar slow waves can be observed but with smaller amplitudes. Accordingly, previous studies relied on a relative rather than absolute threshold[4–6]. Here, we defined slow waves as the waves with absolute peak-to-peak amplitude within the top 10% of all the waves detected for a given EEG electrode and a given participant. On average, the detection threshold was 30 µV (average across N=26 participants and across all electrodes).

Figure 3a shows the average waveform of the slow waves detected on electrode Cz as well as the average waveform of waves detected during sleep recording in another published dataset (N=15 participants)[7]. To compute the average waveform of sleep slow waves, we applied the same algorithm to epochs of 20s scored as NREM2 and NREM3. Only slow waves with peak-to-peak amplitude over 75µV were considered.

We also compared the average waveform of slow waves with task-related Event Related Potentials (ERPs). To do so, we averaged the EEG signal time-locked to stimuli or response onsets at the electrode level. Figure S11a-c shows the average ERP across participants for electrode Cz as well as the scalp topographies of the voltage observed across the scalp at the time of the peak for electrode Cz. Finally, we also compared single-trial voltage values between the average waveforms for slow waves and stimulus-locked or response-locked ERPs (Figure S11d-f, data shown for one participant). Overall, these analyses showed a clear difference between the amplitude, waveform and topographies of slow waves compared to task-related ERPs.

Drift Diffusion Modelling. The Drift Diffusion Model (DDM) assumes that a decision variable noisily accumulates evidence from a starting point (z) with drift rate (v) towards one of two boundaries that represent choice alternatives (i.e. 'Go' or 'No-go'; see Figure S7). The decision threshold (a) is the distance between the two boundaries and represents the amount of evidence that must be accumulated before a decision is made. Once the decision variable crosses a decision boundary, a response is made. Five parameters were fitted using a DDM approach: the participants' initial bias for one of the two responses (decision bias, z), drift rates for Go and NoGo responses (v_{Go} and v_{NoGo}), the decision threshold (a), the non-decision time parameter (t). The last parameter, t, captures extra-decisional components, including stimulus encoding, response preparation and execution. We also extracted the drift rate bias (v_{Bias}) as the difference between the absolute values of v_{Go} (positive) and v_{NoGo} (negative). We performed a model selection based on the Deviance Information Criteria (DIC), which assess goodness of fit while accounting for model complexity in hierarchical models[8]. With posterior predictive checks, we confirmed that our DDM was able to generate simulated behavioural data that are similar to the recorded data (Figure S8; based on the Fz model). For this check, we simulated 100 datasets based on the posterior distributions of HDDM parameters.

Statistics. A cluster-permutation approach (derived from [9]) was applied to identify significant clusters in topographical maps. Candidate clusters were defined as neighbouring electrodes with a p-value below a threshold (called "cluster alpha") of 0.025. For each candidate cluster, we computed the sum of the t-values for all the electrodes belonging to the cluster (which we will refer to as the "cluster statistics"). We then created permuted datasets by permuting the labels of the predictor within each subject, each task and each electrode (N=1,000 permutations). For each of these permuted datasets, we also identified the candidate cluster with maximal absolute cluster statistics. The cluster statistics from permutations formed a null distribution, against which we compared the cluster statistics from the real dataset. Clusters (real and permuted) with positive and negative cluster statistics were compared separately. A Monte-Carlo p-value was derived from this comparison ($p_{cluster}<0.05$ means that a negative cluster has a cluster statistics below the 5th percentile of the permuted distribution and that a positive cluster has a cluster statistics above the 95th percentile of the permuted distribution). In cases where several cluster-permutations were performed in the same analysis (Fig. 5 and 6), we corrected the Monte-Carlo p-values of the real clusters with the Bonferroni method.

References:

1. Mrazek, M. D., Phillips, D. T., Franklin, M. S., Broadway, J. M. & Schooler, J. W. Young and restless: validation of the Mind-Wandering Questionnaire (MWQ) reveals disruptive impact of mind-wandering for youth. *Frontiers in Psychology* **4**, (2013).
2. van Kempen, J. *et al.* Behavioural and neural signatures of perceptual decision-making are modulated by pupil-linked arousal. *eLife* **8**, (2019).
3. Iber, C., Ancoli-Israel, S., Chesson, A. & Quan, S. The AASM Manual for the Scoring of Sleep and Associated Events: Rules, Terminology and Technical Specifications. (2007).
4. Hung, C.-S. *et al.* Local experience-dependent changes in the wake EEG after prolonged wakefulness. *Sleep* **36**, 59–72 (2013).
5. Bernardi, G. *et al.* Neural and Behavioral Correlates of Extended Training during Sleep Deprivation in Humans: Evidence for Local, Task-Specific Effects. *Journal of Neuroscience* **35**, 4487–4500 (2015).
6. Quercia, A., Zappasodi, F., Committeri, G. & Ferrara, M. Local Use-Dependent Sleep in Wakefulness Links Performance Errors to Learning. *Frontiers in Human Neuroscience* **12**, (2018).
7. Legendre, G., Andrillon, T., Koroma, M. & Kouider, S. Sleepers track informative speech in a multitalker environment. *Nature Human Behaviour* **3**, 274–283 (2019).
8. Spiegelhalter, D. J., Best, N. G., Carlin, B. P. & van der Linde, A. Bayesian measures of model complexity and fit. *Journal of the Royal Statistical Society: Series B (Statistical Methodology)* **64**, 583–639 (2002).
9. Maris, E. & Oostenveld, R. Nonparametric statistical testing of EEG- and MEG-data. *J. Neurosci. Methods* **164**, 177–190 (2007).

140 **Supplementary Table 1. Summary of Linear Mixed-Effects Models**

Figure	Predicted Variable X	Level	Predictor Of Interest	Model 0	Model 1
2a-c	False Alarms, Misses, Reaction Times	Probe	Mental State (MS)	X ~ 1 + Task + (1 | Subject)	X ~ 1 + Task + MS + (1 | Subject)
2d-e	Vigilance Scores, Pupil Size	Probe	Mental State (MS)	X ~ 1 + Task + (1 | Subject)	X ~ 1 + Task + MS + (1 | Subject)
N/A	Pupil Size	Probe	Vigilance Ratings (Vig)	X ~ 1 + Task + (1 | Subject)	X ~ 1 + Task + Vig + (1 | Subject)
N/A	Vigilance Scores	Probe	Slow Wave (SW) Properties (density, amplitude, upward slope and downward slope; average across electrodes)	X ~ 1 + Task + (1 | Subject)	X ~ 1 + Task + SW + (1 | Subject)
N/A	Pupil Size	Probe	SW Properties (density, amplitude, upward slope and downward slope; average across electrodes)	X ~ 1 + Task + (1 | Subject)	X ~ 1 + Task + SW Properties + (1 | Subject)
4*	Mental State (binary contrast: MW vs ON; MB vs ON and MB vs MW).	Probe	SW Properties (density, amplitude, downward slope and upward slope per electrode)	X ~ 1 + Task + (1 | Subject)	X ~ 1 + Task + SW Properties + (1 | Subject)
5*	False Alarms, Misses, Reaction Times	Trial	SW (presence or absence)	X ~ 1 + Task + (1 | Subject)	X ~ 1 + Task + SW + (1 | Subject)
6*	a, t, z, v_{Go}, v_{NoGo}, vBias	Subject	SW (presence or absence)	X ~ 1 + Task + (1 | Subject)	X ~ 1 + Task + SW + (1 | Subject)

141
142 **: Analyses corrected for multiple comparison (see Online and Supplementary Methods).*
143

Supplementary Table 2. Effect of normalisation on behavioural analyses

		Normalised	Before Normalisation
Misses (%) in Go trials	State	**$\chi^2(2)=33.4$ (***)**	**$\chi^2(2)=36.0$ (***)**
	MW vs ON	**-0.0096 [-0.015, -0.0041]**	**-0.011 [-0.016, -0.0052]**
	MB vs ON	**-0.023 [-0.032, -0.015]**	**-0.023 [-0.032, -0.015]**
	MB vs MW	**-0.014 [-0.022, -0.0055]**	**-0.013 [-0.021, -0.0047]**
False alarms (%) in NoGo trials	State	**$\chi^2(2)=88.5$ (***)**	**$\chi^2(2)=115.9$ (***)**
	MW vs ON	**-0.24 [-0.29, -0.19]**	**-0.20 [-0.24, -0.17]**
	MB vs ON	**-0.20 [-0.26, -0.19]**	**-0.17 [-0.23, -0.12]**
	MB vs MW	0.064 [-0.014, 0.14]	0.028 [-0.028, 0.084]
RT (s) in Go trials	State	**$\chi^2(2)=33.4$ (***)**	**$\chi^2(2)=16.9$ (**)**
	MW vs ON	-0.0005 [-0.013, 0.011]	-0.0025 [-0.0096, 0.0045]
	MB vs ON	**0.039 [0.022, 0.057]**	**0.019 [0.0088, 0.030]**
	MB vs MW	**0.040 [0.022, 0.058]**	**0.022 [0.011, 0.032]**

*The analyses of the effect of mental states (model comparisons and post-hoc contrasts) were consistent even after normalizing Misses, False alarms and Reactions Times (RT) for each participant by the average obtained on ON probes ("Normalised" column). The "State" row shows the result of the likelihood ratio test (chi-squared value). Stars denote the corrected significance level (Bonferroni correction for 6 likelihood ratio tests: ***: $p<0.001$, **: $p<0.01$, *: $p<0.05$). The estimates of the post-hoc contrasts (MW vs ON, MB vs ON, MB vs MW) obtained from the mixed effect models are also reported, with the corresponding 95% confidence intervals. Bold fonts signal the significant results ($p<0.05$ for model comparisons, or confidence intervals excluding 0 for the post-hoc contrasts).*

Supplementary Table 3. Effect of different pre-probe window sizes on behavioural analyses

		20s before Probes	10s before Probes
Misses (%) in Go trials	State	**χ^2(2)=36.0 (***)**	**χ^2(2)=31.3 (***)**
	MW vs ON	**-0.011 [-0.016, -0.0052]**	**-0.012 [-0.019, -0.0037]**
	MB vs ON	**-0.023 [-0.032, -0.015]**	**-0.033 [-0.045, -0.021]**
	MB vs MW	**-0.013 [-0.021, -0.0047]**	**-0.021 [-0.033, -0.0096]**
False alarms (%) in NoGo trials	State	**χ^2(2)=115.9 (***)**	**χ^2(2)=55.97 (***)**
	MW vs ON	**-0.20 [-0.24, -0.17]**	**-0.20 [-0.25, -0.15]**
	MB vs ON	**-0.17 [-0.23, -0.12]**	**-0.14 [-0.22, -0.062]**
	MB vs MW	0.028 [-0.028, 0.084]	0.061 [-0.018, 0.14]
RT (s) in Go trials	State	**χ^2(2)=16.9 (**)**	**χ^2(2)=8.42** (ns)
	MW vs ON	-0.0025 [-0.0096, 0.0045]	0.0026 [-0.0066, 0.012]
	MB vs ON	**0.019 [0.0088, 0.030]**	**0.020 [0.0064, 0.034]**
	MB vs MW	**0.022 [0.011, 0.032]**	**0.018 [0.0038, 0.031]**

*The analyses of the effect of mental states (model comparisons and post-hoc contrasts) were replicated using a shorter window of 10s (right column) instead of 20s before probe onsets (left column). Likelihood Ratio Tests are reported for the effect of State on the correctness for Go and NoGo trials as well as the Reaction Times (RT) for Go Trials. Stars denote the corrected significance level (Bonferroni correction for 6 comparisons: ***: p<0.001, **: p<0.01, *: p<0.05). The estimates for the post-hoc contrasts and the corresponding 95% confidence intervals are also shown. Bold fonts signal the significant results (p<0.05 for model comparisons, or confidence intervals excluding 0 for the post-hoc contrasts).*

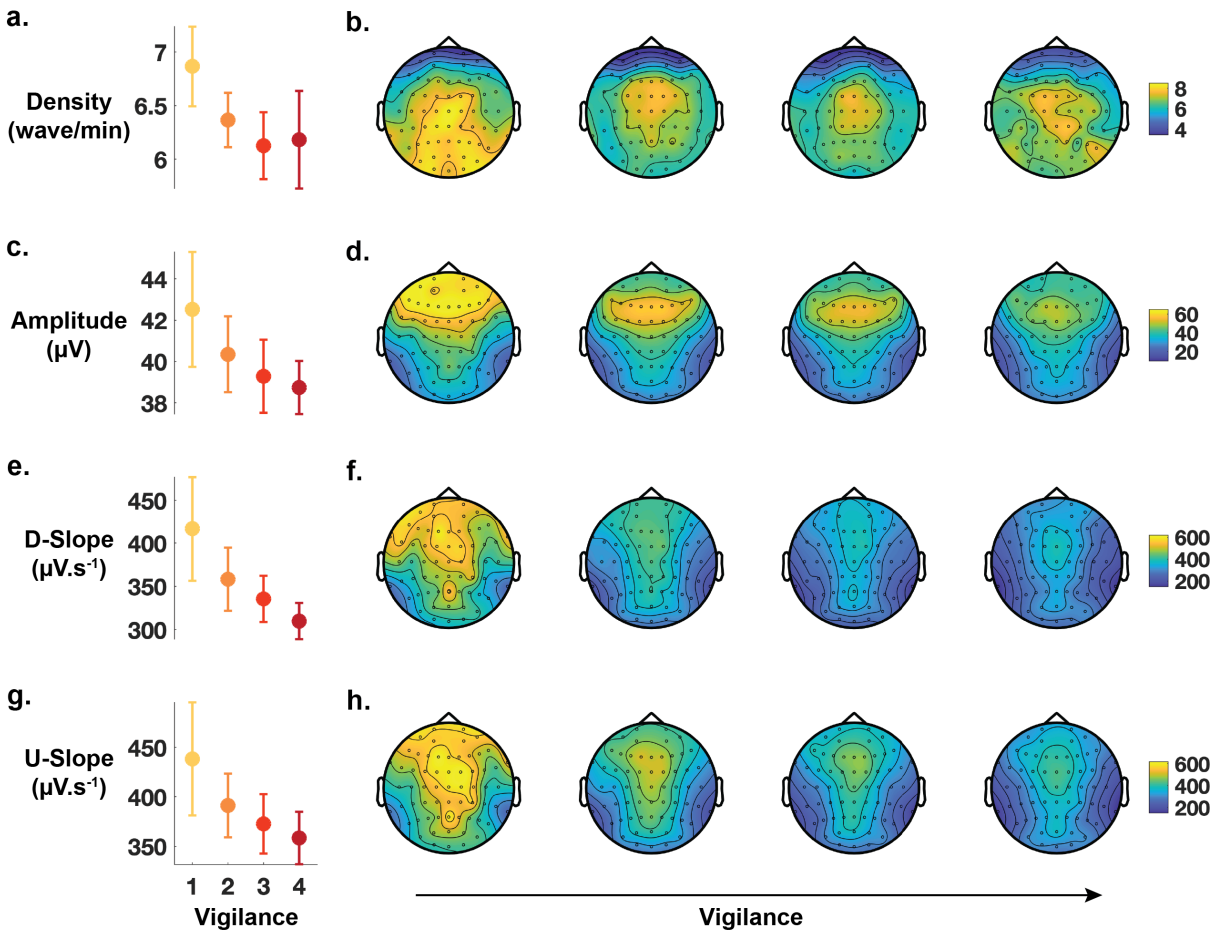

Supplementary Figure 1. Sleepiness is associated with more, larger and steeper slow waves

Slow waves detected within 20s of probes' onset were separated according to participants' vigilance ratings (from 1 (extremely sleepy) to 4 (extremely alert)) provided after each probe. The density (a), amplitude (c), downward slope (D-Slope, e) and upward slope (U-Slope, f), averaged across participants and electrodes, are shown with error-bars showing the standard-error-of-the-mean across participants. Topographies of the average density (b), amplitude (d), downward slope (f) and upward slope (h) are also shown for the different vigilance levels.

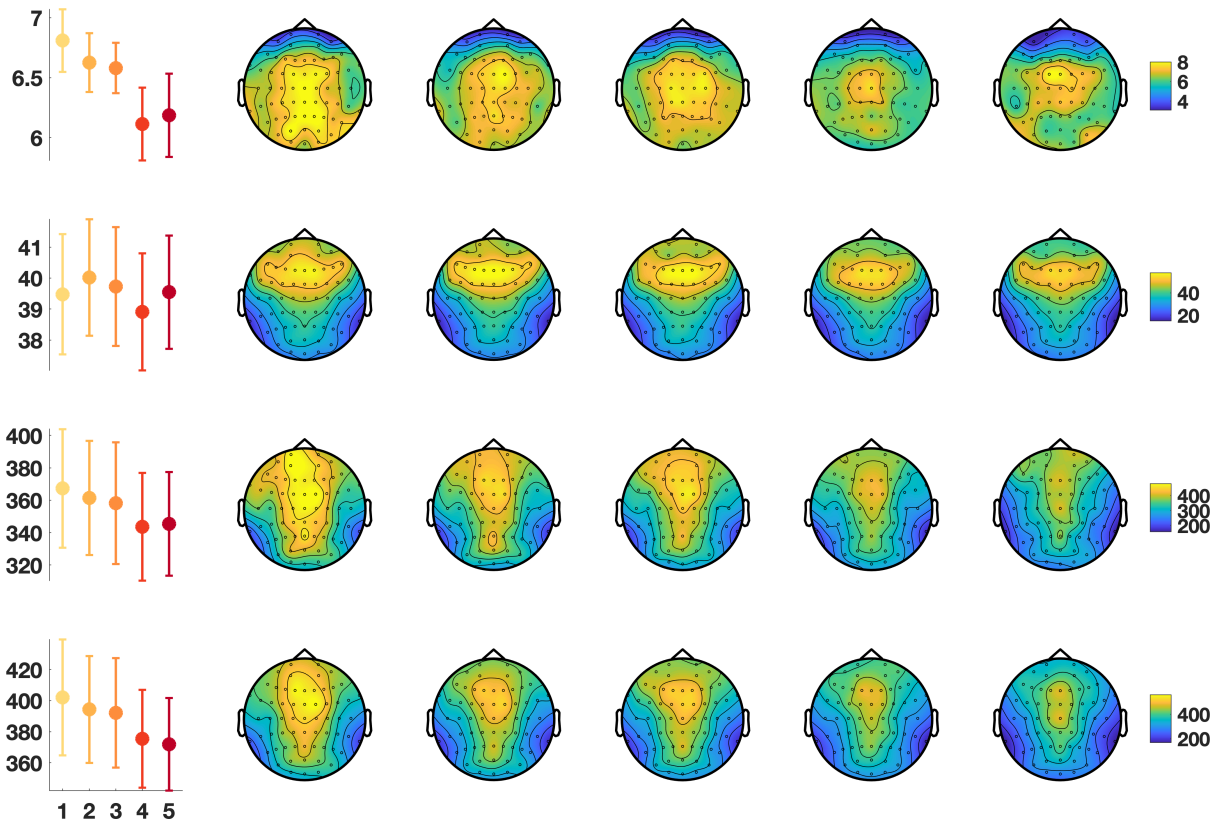

Supplementary Figure 2. A reduction in pupil size is associated with more, larger and steeper slow waves

Slow waves detected within 20s of probes' onset were separated according to participants' pupil size (binned, see Methods) computed on the same window. The density (a), amplitude (c), downward slope (D-Slope, e) and upward slope (U-Slope, f), averaged across participants and electrodes, are shown with error-bars showing the standard-error-of-the-mean across participants. Topographies of the average density (b), amplitude (d), downward slope (f) and upward slope (h) are also shown for the different pupil size bins.

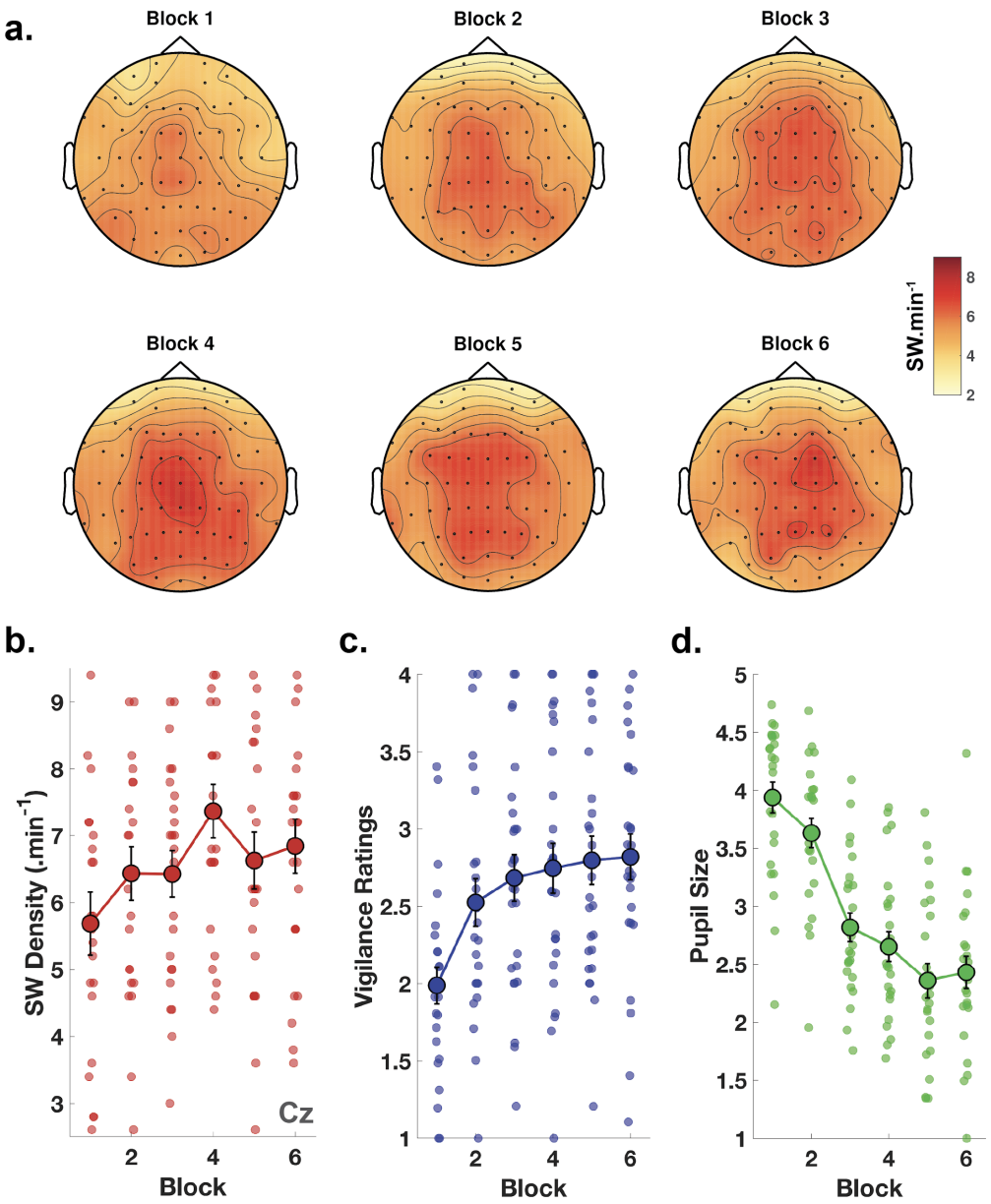

Supplementary Figure 3. Slow waves increase with time spent on task

(a) Topographies of the temporal density of slow waves (slow waves per minute, averaged across all 26 subjects). An increase in the number of slow waves, maximal over central electrodes, can be seen from the first to the last experimental block. (b-d) Slow wave density for electrode Cz (b), vigilance ratings (c) and pupil size (d) averaged within each block. Connected larger dots show the average across participants (error-bars: SEM). Individual semi-transparent circles show individual subjects.

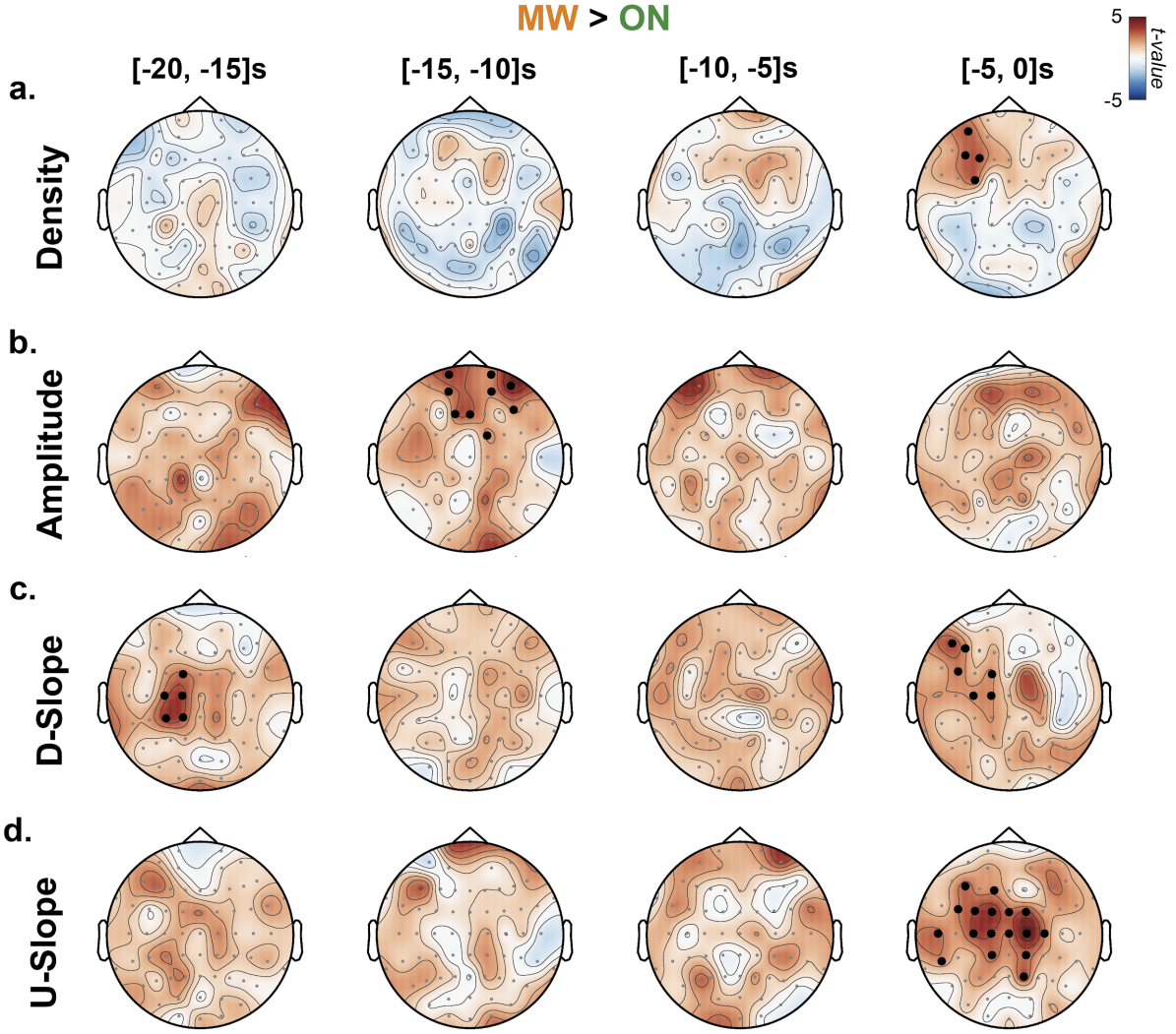

Supplementary Figure 4. Spatiotemporal dynamics of the effect of slow-waves properties on mental states (MW vs ON).

*Mixed-Effects Models were used to quantify the impact of slow-wave properties (**a**: Density; **b**: Amplitude; **c**: Downward Slope (D-Slope); **d**: Upward Slope (U-Slope)) on mental states as in Figure 4. Slow waves were detected on 4 different windows: [-20, -15]s, [-15, -10]s, [-10, -5]s and [-5, 0]s before probe onsets. Slow-wave properties were extracted for each electrode and used to predict the MW vs ON contrast. Topographies show the scalp distribution of the t-values associated with each slow-wave parameter and electrode. Black dots denote significant clusters of electrodes ($p_{cluster}<0.05$ corrected for 48 comparisons (Figure S4-6) using a Bonferroni approach).*

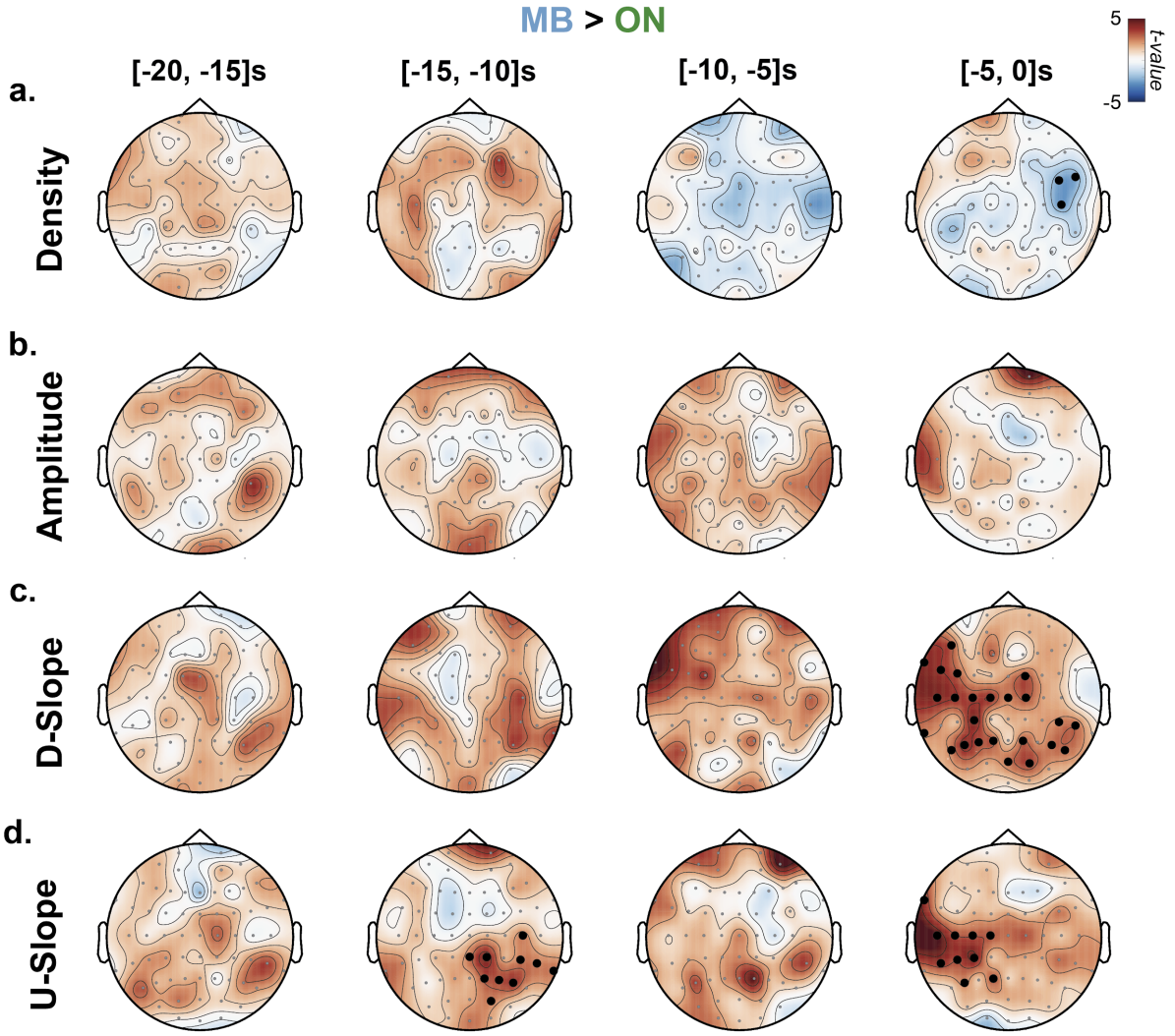

Supplementary Figure 5. Spatiotemporal dynamics of the effect of slow-waves properties on mental states (MB vs ON).

Same format as in Supplementary Figure 4.

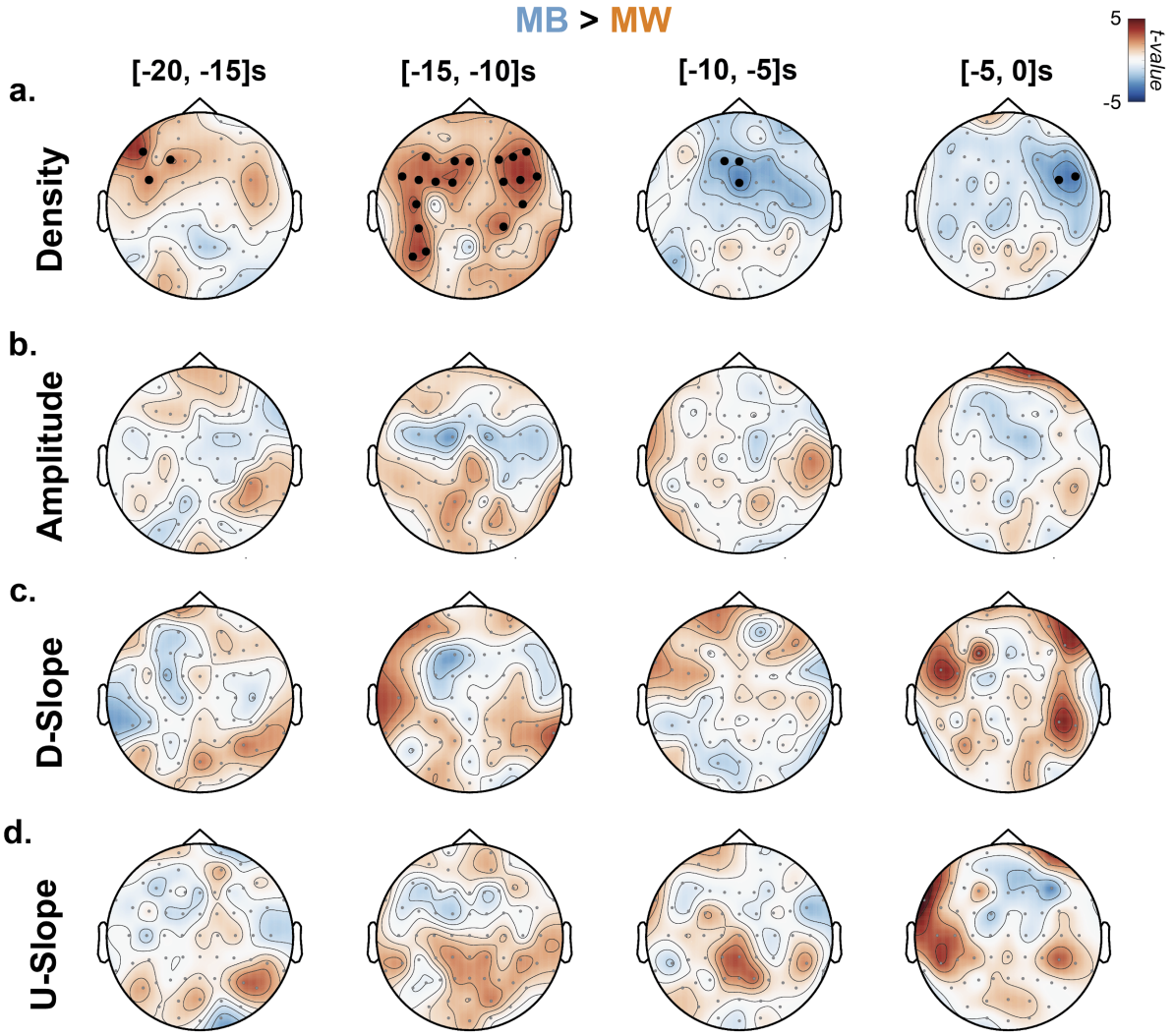

Supplementary Figure 6. Spatiotemporal dynamics of the effect of slow-waves properties on mental states (MB vs MW).

Same format as in Supplementary Figure 4.

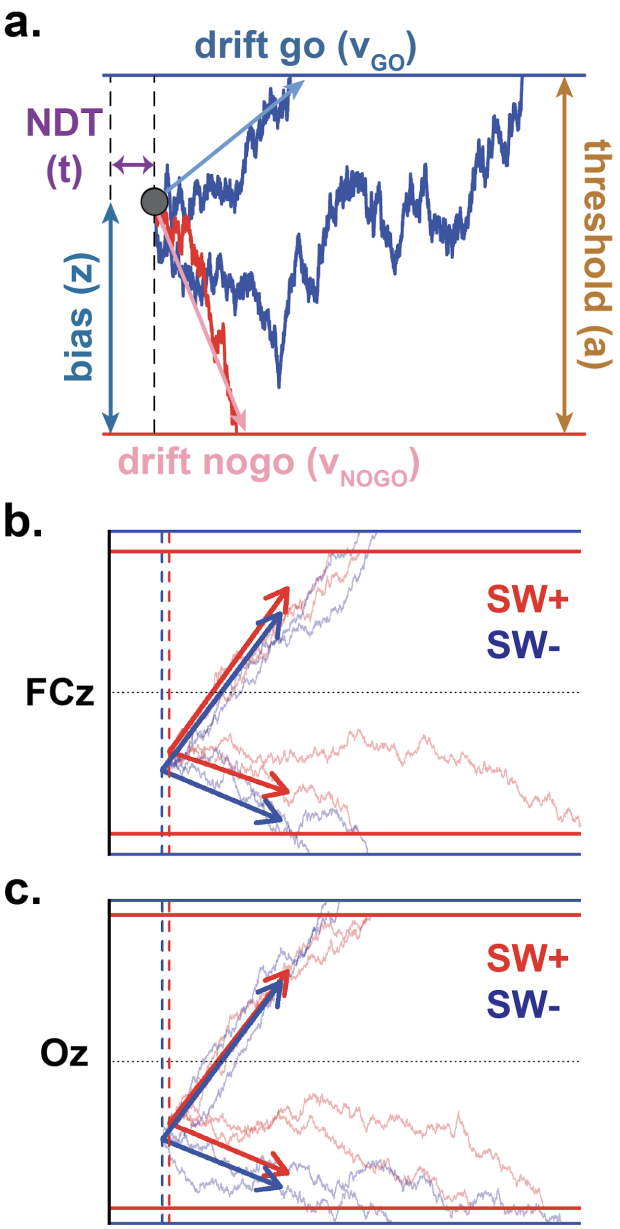

Supplementary Figure 7. Drift Diffusion Modelling

a: *The Go/NoGo tasks were modelled according to the Drift Diffusion Model (DDM, see Online and Supplementary Methods). The following parameters were estimated: threshold (a), non-decision time or NDT (t), bias (z), drift rate for Go trials (v_{Go}), drift rate for NoGo trials (v_{NoGo}). We then also computed the drift bias: abs(v_{Go})-abs(v_{NoGo}). The figure shows a graphical representation of these parameters. Note that here, drift rates for NoGo trials are negative.* ***b-c:*** *Graphical representation of decision processes using the parameters obtained by the DDM for trials with (SW+) or without (SW-) slow waves. The presence or absence of slow waves was determined for each electrode (FCz (b; frontal) and Oz (c; posterior)). Note the reduction in decision threshold, drift rates and bias associated with slow waves but the increase in NDT.*

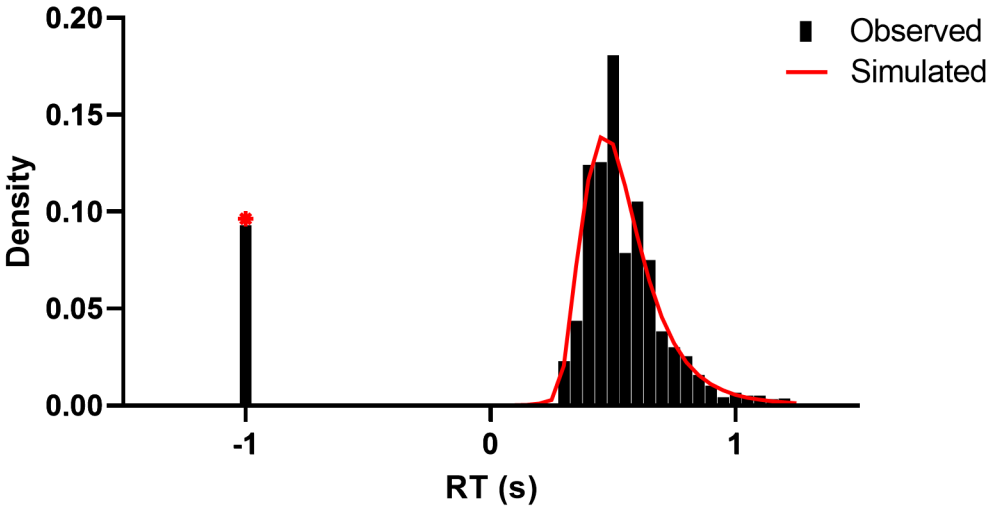

Supplementary Figure 8. HDDM Fit to Behavioural Data

Posterior predictive checks of Go/No-Go DDM fit to the behavioural data. Observed data for all participants (black bars) are plotted underneath model-predicted RT distributions and No-Go choice proportions (red lines). Positive distribution represents the normalised frequency of reaction times (RT) from Go responses. Negative bin at RT=-1 represents the proportion of No-Go responses.

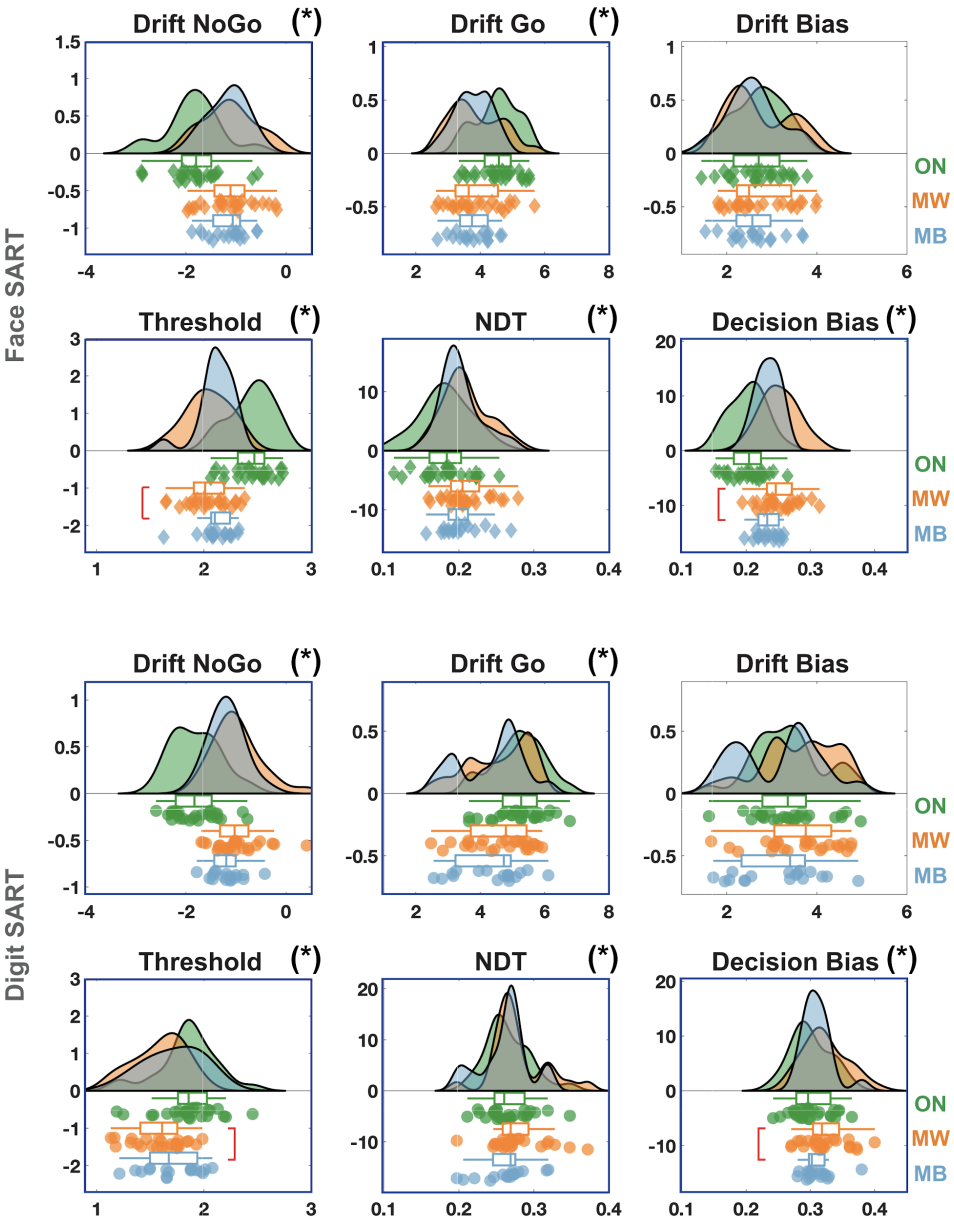

Supplementary Figure 9. Impact of mental states on HDDM parameters.

*Hierarchical Drift Diffusion Modeling (HDDM, see Methods) was applied to the Reaction Times obtained in the Face (top) and Digit (bottom) SART. The parameters were fitted for each task and mental state. Each panel shows the distribution of the estimated variable for individual participants (drift for NoGo and Go trials, drift bias, threshold, non-decision time (NDT) and decision bias; see Methods). For each plot, coloured areas show the smoothed distribution of individual data points (see Methods). Diamonds and circles show individual estimates for the Face and Digit SART respectively. Box plots show the 1st and 3rd quartiles (edges) as well as the median (middle bar). Blue boxes around individual plots and stars next to the titles indicate variables with significant state-effects (model comparison, see Methods; *: p<0.05, Bonferroni correction for 12 comparisons). Significant differences between MW and MB (for threshold and decision bias) are highlighted with red brackets.*

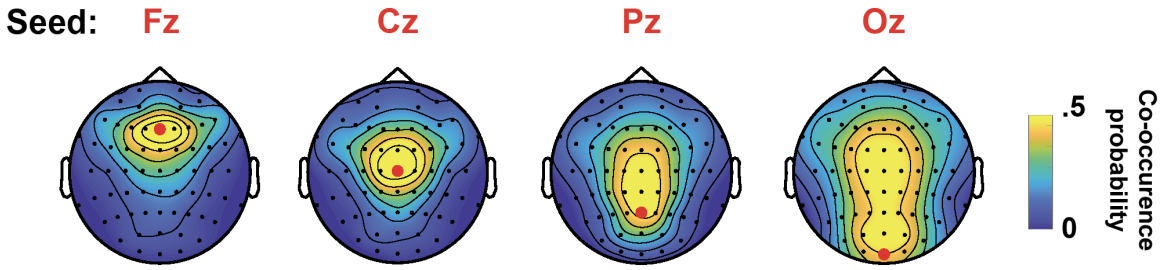

Supplementary Figure 10. Spatial expanse of slow waves

Four seeds electrodes were selected along the scalp midline from the front (Fz) to back (Oz). For each slow wave detected in these seed electrodes, we computed the probability that slow waves were also observed in the other electrodes. The average co-occurrence probability averaged across participants (N=26) is shown for each seed electrode. Note that slow waves detected over Fz tend to co-occur with other slow waves only in a limited number of neighboring frontal electrodes whereas occipital slow waves (Oz) tend to co-occur with other slow waves in both frontal and posterior electrodes (more widespread).

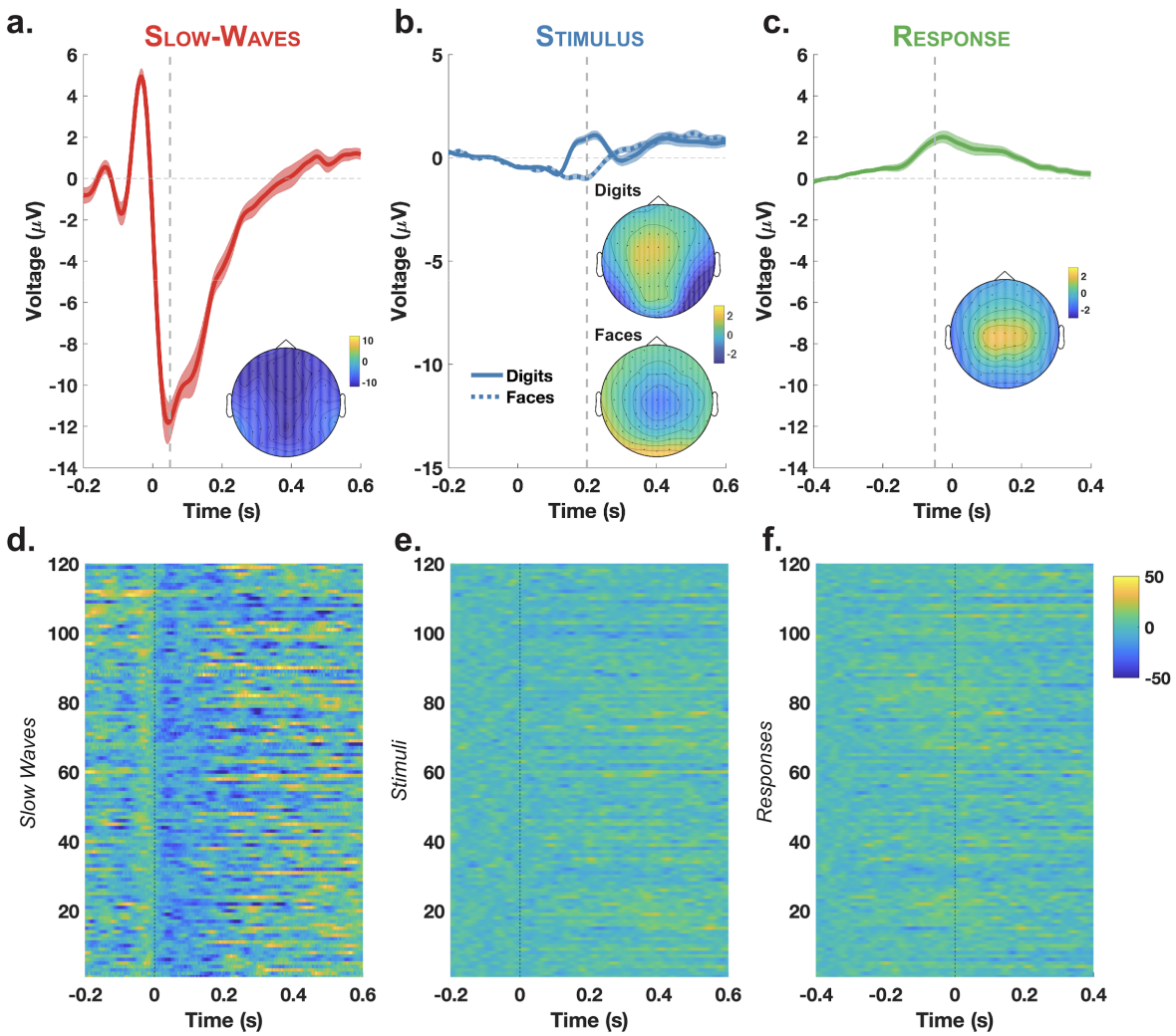

Supplementary Figure 11. Slow waves compared to stimulus and response-locked activity

Event-related potentials averaged over electrode Cz and across participants for slow waves (a), stimulus-locked activity (b) and response-locked activity (c). Slow waves' EEG time courses are aligned with the first negative crossing before the negative peak. Stimulus-locked responses are aligned on the onset of the digit (full line) or face (dotted line) stimuli. Response-locked responses are aligned to the onset of participants' responses. Shaded areas show the SEM across participants (N=26). Insets show the topography of the average voltage at the times shown by the vertical dotted lines (a: 0.05s; b: 0.2s; c: -0.05s), which approximates the absolute maximum of each ERP. (d-f) Voltage of the event-related potentials per trial for one participant. Each row corresponds to (d) an individual slow wave, (e) a stimulus presentation (face or digit), (f) a motor response. We limited the number of rows in (e) and (f) to match the number of detected slow waves (N=120) in (d).

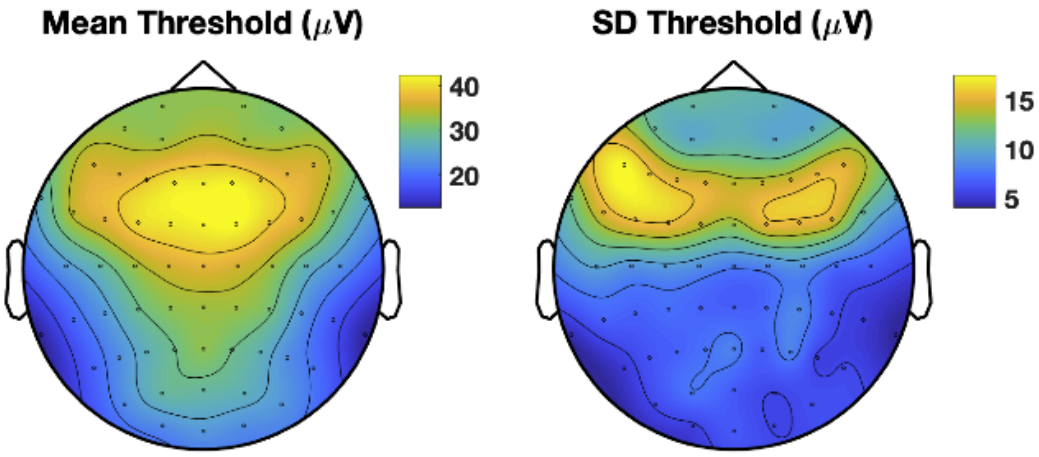

Supplementary Figure 12. Scalp topography of the average and standard-deviation of the slow-wave detection threshold

Only slow waves whose amplitude is within the top-10% of the distribution for each electrode and participant were analysed. The left topography shows the value, in voltage, of this threshold for each electrode, averaged across participants. The right topography shows the standard deviation (SD) of the threshold values across participants.